Article:

Hao, Y., Zhang, H. orcid.org/0000-0002-4241-2359, Zhang, Z. orcid.org/0000-0003-0204-3867 et al. (2 more authors) (2024) Development of Force Sensing Techniques for Robot-Assisted Laparoscopic Surgery: A Review. IEEE Transactions on Medical Robotics and Bionics, 6 (3). 868 - 887. ISSN 2576-3202

https://doi.org/10.1109/tmrb.2024.3407238

Development of Force Sensing Techniques for Robot-Assisted Laparoscopic Surgery: A Review

Yupeng Hao, Han Zhang, Zhiqiang Zhang, Chengzhi Hu, Chaoyang Shi

Abstract— **Robot-assisted laparoscopic surgery (RALS) has been widely investigated and developed as a routine and preferred minimally invasive surgery (MIS) because of enhanced operational precision and dexterity, improved visualization, and reduced surgeon stress and fatigue. However, the lack of force feedback poses challenges to accurate interaction force perception, lowered surgical errors, improved patient safety, and upgraded surgical outcomes. The solutions to force sensing can empower surgeons with a more intuitive and natural surgical experience with accurate perception capacity of interaction forces, efficient motor skill acquisition, enhanced surgical quality, and support the development of high-level techniques for surgical intelligence and autonomy. Although extensive research has been investigated in this field, effective and solid solutions are still unavailable for actual surgical scenarios. This review provides a comprehensive investigation from starting implementations to recent advances in emerging techniques for physical force sensors in laparoscopic surgery and RALS and focuses on the following categories: strain gauge-based, capacitive-based, and optical fiber-based principles. The design of force-sensitive structures from the mechanism perspective has been emphasized to provide possible and valuable design guidance for force sensor implementations with expected performance. Merits and limitations of existing technologies and prospects of new technologies are also discussed.**

Index Terms— **Laparoscopic surgery; Minimally invasive surgery (MIS); Force feedback; Strain gauge sensor; Capacitive sensor; Fiber optic sensor (FOS); Fiber Bragg grating (FBG).**

I. Introduction

Laparoscopic surgery has extensively evolved into a symbolic and routine minimally invasive procedure and is developed as an exceptional alternative to traditional open surgery [1-5]. The associated procedure typically involves performing accessible diagnosis or delicate and complex therapeutic tissue interventions inside the abdominal, thoracic, or pelvic cavities by inserting specialized laparoscopic instruments and an endoscopic camera through small keyhole incisions [6-9]. Leveraging these merits and addressing the limitations associated with manual laparoscopic surgery, RALS has also been emergingly introduced in a master-slave control mode and undergoes rapid development and progressive applications due to its advantages of enhancing surgical precision and dexterity, advancing visualization, reducing surgeon fatigue, and improving patient outcomes [8, 10-13]. However, the absence of force feedback remains a challenging problem for both laparoscopy and RALS and thus poses significant challenges to enhancing surgical outcomes, improving patient safety, shortening the learning curve, and further restricting the development of the associated techniques for intelligence and autonomy of surgical robots [14-16]. According to the statistics and analysis of surgical trainees' operations, the previous study found that around 56% of surgical consequential errors are produced by exerting either excessive or insufficient forces for laparoscopic cholecystectomy [17, 18]. The tool-tissue interaction forces perceived by surgeons are typically amplified and even distorted, which are attributable to the induced internal friction forces inside instruments and the disturbance forces from the internal surrounding tissues and organs by the leverage amplification effect [19, 20]. Furthermore, the gripping forces felt by surgeons' hands are typically 2 to 6 times larger than the actual distal instrument grasping forces [20]. The utilization of haptic feedback and pseudo-haptic feedback can offer surgeons a more intuitive and natural surgical experience by providing physical tactile sensations and auditory, visual, or other simulated tactile sensations, respectively [21-23]. Accurate and robust force sensing technologies are crucial as the premise for (pseudo) haptic feedback [24]. These technologies could enable surgeons to accurately perceive interaction forces, explore anatomical structures, and identify tissue properties during tissue interventions [25, 26]. These merits support suppressing the possibility of surgical errors, enhancing surgical quality, increasing the speed of skill acquisition, and developing high-level robot-associated techniques for surgical autonomy [27-29].

The mainstream RALS provides tissue deformation information based on visual feedback as an alternative to help surgeons estimate the interaction status between surgical instruments and tissues, which significantly limits safety and effectiveness during surgical operations [18]. The sensorless method typically develops force-estimation algorithms based on the vision feedback and mechanical interaction models. It avoids the problems of increased costs and original function destruction of the instruments but necessitates a lengthy and expensive training phase [30-32]. Consequently, more precise

Manuscript received 24 Feb 2024. This work was supported in part by the National Natural Science Foundation of China under Grant 62211530111 and Grant 92148201, Technology Program Project of Shaoxing City under Grant 2023A14016, Science and Royal Society under IEC\NSFC\211360, and Graduate Research Innovation Project by Tianjin Education Commission under Grant 2022BKY075. Corresponding author: C. Shi (chaoyang.shi@tju.edu.cn)

Y. Hao, H. Zhang and C. Shi are with the Key Laboratory of Mechanism Theory and Equipment Design of Ministry of Education, School of Mechanical Engineering, Tianjin University, Tianjin 300072, China. Z. Zhang is with School of Electronic and Electrical Engineering, University of Leeds, Leeds, LS2 9JT, UK. C. Hu is with Guangdong Provincial Key Laboratory of Human-Augmentation and Rehabilitation Robotics in Universities, Department of Mechanical and Energy Engineering, Southern University of Science and Technology, Shenzhen, 518055, China. This work is also supported by International Institute for Innovative Design and Intelligent Manufacturing of Tianjin University in Zhejiang, Shaoxing 312000, CN.

models and advanced algorithms are needed to enhance the accuracy of force estimation and reduce computational time [19]. In contrast, physical sensing techniques embrace the more significant potential to provide multiple dimensional measurements in real-time, maintain higher reliability, and improve surgical procedures' accuracy, efficiency, and safety [23, 24]. Therefore, various force-sensing techniques based on physical sensors for RALS have attracted extensive investigation.

This article comprehensively reviews the early and starting implementations as well as recent progress and advances of various force sensors for RALS. Section II reviews the existing and typical force sensors based on strain gauge, capacitance, and optical fibers. The characteristics and performance of these sensor prototypes and their integrations in different locations along the surgical instruments are compared, as presented in detailed tables and figures. The advantages and limitations of existing technologies for force sensors are discussed. This review further analyzes the design of force-sensitive structures and outlines their correlation with sensor performances regarding measurement dimension, accuracy, resolution, and decoupling ability. The potential of the force-sensitive structure design from the mechanism perspective to provide a part of the framework or guidelines for force sensor developments in RALS is also emphasized.

Literature research was performed on IEEE Xplore, ScienceDirect, Web of Science, Springer, and PubMed for articles related to the design and development of force-sensing techniques for RALS from 1994 to 2023 utilizing the keywords 'laparoscopic surgery', 'force sensor', 'haptic feedback', 'surgical robot', and similar terms. The literature relevance was taken as the inclusion criterion. Primary screening based on the title and abstract, followed by detailed full-text screening, ensured that the literature was directly related to the topic of 'Force sensors for RALS'. Moreover, literature with a small sample size, poor methodology, or unreasonable research design and without peer-reviewed academic journals was excluded to ensure academic credibility and reliability.

II. Sensing Technologies

A. Overview of the Development of Force Sensors for RALS

1) **Analysis of Design Requirements**

To achieve higher accuracy and reliability in force sensing and satisfy the clinical requirements of the sensing instruments, the force sensor design for RALS requires comprehensive consideration of essential factors such as sensing DoFs, sensitivity, size, packaging, sterilization, and so on. The following contents outline the primary design requirements.

a) Although higher dimensional force sensors can provide surgeons with a more authentic sense of presence, the grasping force, instrument force, and axial torque are the most relevant DoFs to provide effective force sensing for RALS [18, 19], as illustrated in Fig. 1.

b) There exists a trade-off between structural stiffness and sensor sensitivity. In most RALS applications, a measurement range of ±10N in all directions and 0-10 N for grasping, as well as a resolution of 0.2 N are considered sufficient [33, 34], as the human just-noticeable difference (JND) is 10% within [0.5 N, 200 N] and increases to 15-27% below 0.5 N.

c) The sensors should be miniatured to facilitate compact integration with surgical instruments and reduce interferences in their original functions [35, 36]. Furthermore, the sensor packaging demands effective and practical insulation against static electricity, shielding against electromagnetic interference (EMI), and secure sealing to prevent foreign objects [37]. The adopted materials also have to meet biocompatibility requirements [38].

d) Surgical instruments require experiencing strict cleaning and sterilization procedures before re-usage [37]. Therefore, the sensors should be specially designed to avoid damage to the signal conditioning electronics, wire insulation, bonding, and coatings during sterilization procedures with 120-135°C, 207 kPa, and 100% humidity for 15-30 minutes [38, 39].

e) The currently available robotic instruments are expensive and have a compulsory limit of 10-15 uses [40, 41]. Therefore, modular mounting sensors are desirable for force feedback in RALS [18].

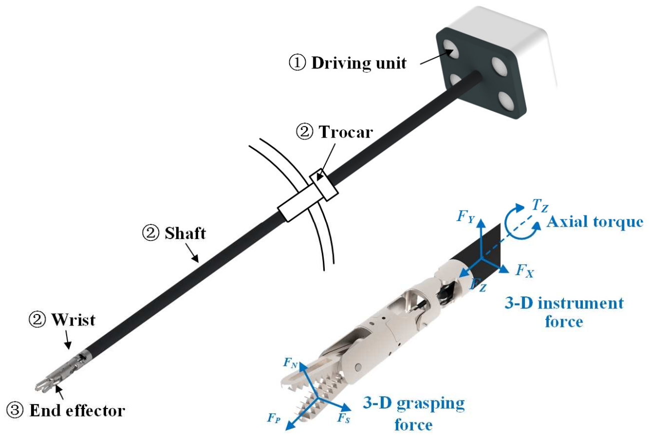

Fig. 1. Integration locations and detailed DoF distribution of the force-sensing techniques for RALS.

2) **Summary of Sensing Principles and Integration Locations**

To promise different sensing requirements and target various usage scenarios, force sensing techniques for RALS adopted various sensing principles [42], including the strain gauge [43-46], capacitance [47-50], piezoelectricity [51-53], and optical fibers [54-62]. Their working principles, merits, and disadvantages are summarized in Table I. Piezoelectric sensors are not discussed in the following sections due to their lack of static force measurement capability and limited usage in RALS.

Various sensors have been integrated into different locations of the surgical robot to satisfy different requirements [7]. This survey analyses the advantages and disadvantages of integrating force sensors in the proximal driving unit, the instrument shaft (wrist, trocar), and the distal end effector (Fig. 1), respectively. Their corresponding applicability and performance in laparoscopic surgical robots are discussed

TABLE I
SUMMARY OF SENSING PRINCIPLES, ADVANTAGES AND DISADVANTAGES OF DIFFERENT SENSING METHODS

Force sensing principles		Description	Advantages	Disadvantages
Strain-gauge-based [43-46]		Resistive strain effect of metals or the piezoresistive effect of semiconductor elements	• High accuracy • Compact size • High reliability • Cost-effectiveness	• Complex circuit • Susceptible to EMI
Capacitive based [47-50]		Capacitance variation due to the distance or overlap area change between two electrodes	• High sensitivity and resolution • No drift • Long time stability	• Limited measurement range • Edge effect • Parasitic capacitance
Piezoelectric based [51-53]		The piezoelectric effect that converts strain or force to electrical change	• High-frequency response • High dynamic range • Excellent accuracy	• Not suitable for static force sensing
Optical fiber-based	**Light intensity modulation (LIM) [54-56]**	Voltage or current variation due to force-induced intensity change	• Simple structure • Cost-effectiveness • Ease of signal interpretation	• Low robustness
	Phase modulation [57-59]	Relative phase shift between light beams due to the force or displacement	• High sensitivity • Wide dynamic range • Rapid response	• Require expensive and high-quality light source
	Wavelength modulation [60-62]	Grating's reflecting wavelength shift under strain and temperature	• Excellent sensitivity • High linearity • Support multiple-point measurement	• Temperature sensitivity • Require expensive optical interrogation

below. The proximal sensors integrated at the driving unit are located away from the surgical operation sites [40, 63]. These sensors typically have fewer requirements in terms of size, weight, sterilizability, and biocompatibility. However, they mainly indirectly measure the interaction forces at the distal end of the instruments, resulting in decreased measurement accuracy due to friction, hysteresis, disturbance forces, and leverage effects. The distal sensors assembled on the instrument shaft generally achieve high sensitivity in radial force measurement [64-67]. However, the sensor's outer diameter should be smaller than that of the surgical instrument (typically less than 10 mm), and the internal structural design of the sensor requires reserved channels to carry driving cables and surgical instruments. The sensors integrated into the end effectors (graspers and scissors) realize the direct force detection between tissues and instruments [68-71]. This configuration allows the sensor to be independent of friction and inertial forces, allowing its highest measurement accuracy among all configurations. However, these sensors suffer from stringent requirements to ensure the sensor's performance and restore the original functions of the instruments.

B. Strain Gauge-based Force Sensing

The integration of strain gauges with surgical instruments can be mainly categorized into two types: those integrated with the instrument shafts or driving units to measure instrument and grasping forces, as well as those integrated into the graspers to directly detect grasping forces.

Bicchi et al. from the University of Pisa first introduced strain gauge-based sensors for laparoscopic instruments in 1996, as illustrated in Fig. 2-a1). They attached two strain gauges to both the inner and outer surfaces of a ring, respectively, and fixed this ring to the driving rod of a commercial instrument for the grasping force sensing. A position-sensing device was employed to measure the angular variation of the grasper jaws, enabling this sensor to help surgeons perceive different tissue stiffness values [72, 73]. Additionally, Prasad et al. [74] adopted four orthogonally placed strain gauges onto a sleeve that could be fitted modularly with laparoscopic instruments to quantify the 2-D radial forces (Fig. 2-a2)). Based on a similar strain gauge arrangement, Mayer et al. developed a sensing instrument and mounted it into a surgical robot system (Fig. 2-a3)), significantly benefiting autonomous surgical planning [75]. However, simultaneously measuring both the grasping and the instrument forces is indispensable for laparoscopic instruments.

To further measure both the grasping and instrument forces, Tholey et al. integrated a resistive sensor and four strain gauges into the jaw and the distal end of the instrument shaft, achieving grasping force detection within [0, 13 N] and 2-D instrument force measurement within [0, 10 N], respectively (Fig. 2-a4)). However, the grasping force perception displayed significant non-linearity and hysteresis [76, 77]. Besides, Dalvand et al. integrated the strain gauges into the proximal end of the instrument driving rod to achieve an indirect and linear measurement of the grasping force (Fig. 2-a5)). However, this approach of directly attaching strain gauges to the instrument shaft induced severe sensing coupling between the grasping and instrument forces [78, 79]. Trejos et al. addressed this problem by employing a specially designed triple-concentric-shaft configuration and realized the decoupling 5-D force/torque (F/T) measurement (Fig. 2-a6)). The inner, middle, and outer shafts of this triple-shaft configuration were equipped with strain gauges to measure the actuation force, radial force, as well as axial force and torque, respectively [80]. However, the accuracy of these sensors was limited by trocar friction, gravity, and inertial forces resulting from directly attaching the strain gauges to the original instruments.

To overcome these limitations, Shimachi et al. proposed a novel force-sensing method termed as Overcoat that can be

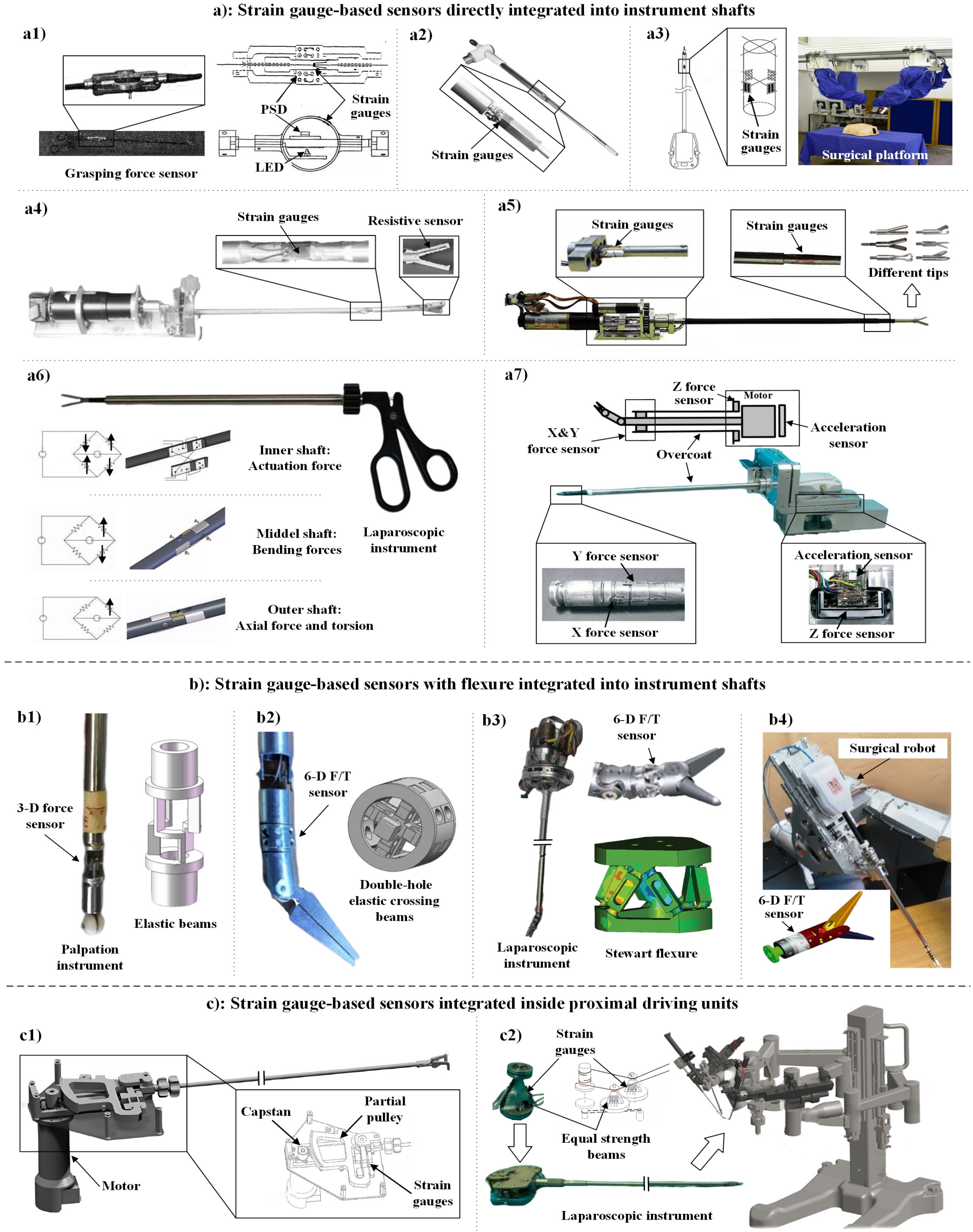

Fig. 2. Strain gauge-based force sensors integrated into shafts (a, b) and driving units (c) of the laparoscopic instruments. a1) Sensing ring fixed on the shaft for grasping force measurement [72], ©1996 IEEE; a2) Modular sleeve with 2-D radial force sensing capacity [74], ©2003 Springer; a3) Sensing instrument with strain gauges attached to the shaft and the surgical platform equipped this instrument [75], © 2006 IEEE; a4) 2-D radial force sensor based on strain gauges and sensing grasper based on a resistive sensor [76], © 2007 IEEE; a5) 3-D sensing instrument for different tips [79], © 2014 John Wiley; a6) 5-D F/T sensor with triple-concentric-shaft configuration [80], © 2009 ASME; a7) 3-D force sensor utilizing the basic type of Overcoat method [83], © 2008 John Wiley and Sons; b1) 3-D force sensor with triple elastic beams [36], © 2015 Emerald Group Publishing Limited; b2) 6-D F/T sensor with double hole elastic crossing beams [85], © 2013 Springer; b3) 6-D F/T force sensor based on the Stewart flexure [88], © 2004 IEEE; b4) 6-D Steward-based sensor of less parasitic effect [67], © 2017 John Wiley and Sons; c1) Sensing pulley for grasping force sensing [96], © 2002 IOS PRESS; c2) Cable tension sensor of multiple-DOF instruments for surgical robot [63], © 2014 John Wiley and Sons. All figures are reprinted with permission of the corresponding references.

categorized into two types: the basic type and the trocar type. The basic type involves placing force sensors between the instrument shaft and an overcoat covering the shaft outside, creating the configuration of triple concentric shafts to measure 3-D forces without interferences from trocar friction or gravity (Fig. 2-a7)). Meanwhile, an acceleration sensor was integrated behind the motor to compensate for inertial forces. This sensing instrument was integrated into the Da Vinci Surgical System and achieved high accuracy values of 0.1 N in both the x and y directions as well as 0.2 N in the z direction [81-83]. Besides, the trocar type integrated sensors into a double-layer trocar to avoid the modification of the instrument and reduce the cost. However, this type suffered a poor absolute accuracy of 0.3 N with a sensitivity of 0.05 N, and the vibration of the instrument shaft negatively impacted inertial force cancellation [84].

In addition to directly utilizing the instrument shafts as sensing structures, specially designed flexible structures for multidimensional sensors were introduced to offer greater compactness, improved performance, and decoupling measurement. Li et al. proposed a 3-D palpation force sensor that utilized a tripod flexure consisting of three elastic beams [36]. Each flexible beam comprised one horizontal beam and two vertical beams with a strain gauge attached to the lower vertical beam, as illustrated in Fig. 2-b1). This sensor was integrated into a palpation instrument shaft and suffered a limited radial force measurement range of [-1.5 N, 1.5 N]. Jiang et al. further proposed a 6-D sensor composed of two double-hole parallel crossing elastic beams with 32 strain gauges (Fig. 2-b2)). This sensor achieved an enhanced measurement range of [0, 10 N] and [0, 150 N·mm] and 6-D F/T decoupling sensing with a maximum coupling error of 4.29% by employing a clearance fit between the elastomer and the shell [85-87]. However, high-dimensional force sensors based on the traditional crossbeam structure need to attach lots of strain gauges, thereby increasing the complexity of sensor fabrication and integration.

Furthermore, the mechanism-based approach, applying the parallel mechanism platform as the sensing structure, reduces the number of strain gauge patches and allows larger central channels for surgical tools and cables. Seibold et al. [88-91] affixed 6 strain gauges into the links of a Stewart-based structure to realize 6-D F/T sensing and integrated this sensor into the wrist of a wire-driven laparoscopic surgical instrument (Fig. 2-b3)). Nevertheless, this sensor suffered an evident crosstalk due to the parasitic motion of the flexible links. Li et al. [67, 92] improved the 6-D Stewart-based sensor by increasing the inertia moment of the links to minimize the parasitic effect and mounting 12 strain gauges onto each front and back side of six links (Fig. 2-b4)). The ex-vivo palpation experiments demonstrated that this sensor achieved excellent linearity, low crosstalk of 5%, and low hysteresis of 2.5%. Matich et al. developed a 6 F/T Stewart-based miniaturized sensor by rolling a steel plate with 12 strain gauges to form a hexapod structure [93, 94]. This sensor achieved measuring ranges of 4 N and 66 mNm with crosstalk smaller than 2.76 %.

Sensors integrated into the driving unit are more accessible to design and assemble than in other integrated locations because of the larger available size. Hu et al. affixed strain gauges to the handle of a handheld disposable laparoscopic instrument for measuring grasping force, but the accuracy was limited by hand tremors [95]. Furthermore, Brown et al. presented a sensing pulley with two strain gauges to indirectly measure the 1-D grasping force (Fig. 2-c1)). The pulley was connected to the cable at the driving unit of a handheld automated MIS instrument and achieved outstanding static and dynamic performance in ex-vivo experiments [96, 97]. Moreover, He et al. developed a force sensor utilizing an equal-strength cantilever beam with four strain gauges [63]. This sensor was installed on the cable-winding wheels at the driving unit of a robot-assisted laparoscopic instrument to measure the cable tension and further calculate the grasping force and 3-D instrument forces (Fig. 2-c2)). This sensing technique achieved an impressive resolution of 0.04 N. However, the integration into the driving unit resulted in poor measurement accuracy owing to friction between the cable and the instrument wrist. Matich et al. developed three strain gauge-based axis force sensors and connected them between the motors and driving rods to achieve an indirectly estimation of 3-D interaction force. A longitudinal vibration strategy was employed to mitigate the impact of friction and enhance sensing precision [98].

Integrating force sensors into the effectors effectively mitigates performance degradation caused by friction, rebound, and hysteresis, thereby enhancing sensing accuracy. Nevertheless, this approach necessitates structural modifications to the grasper without affecting its original functions. Tholey et al. integrated a piezoresistive sensor (Fig. 3-a1)) with 3-D force measurement capability onto the back part of automated laparoscopic grasping jaws to measure 3-D grasping forces [99, 100]. Fischer et al. [101] developed a 3-D sensing grasper and integrated two sets of strain gauges onto the locations with maximum strain values of each jaw to detect axial and bending forces, respectively (Fig. 3-a2)). However, these approaches increased the graspers' size and inevitably impacted their original function.

Therefore, flexure-based sensors were adopted to reduce the grasper sizes, enhance sensor performance (e.g. sensitivity), and retain the original functions of graspers. Stephan et al. proposed a novel MIS grasper comprising planar elastic beams in three orthogonal directions and strain gauges to detect the grasping and 3-D instrument forces (Fig. 3-b1)). However, the complex design of the sensor led to complicated assembly and significant measurement errors, while the smooth surfaces resulted in impaired grasping capacity [102]. Hong et al. further integrated two flexure hinges into the proximal end of the grasper, preserving the working surface of the grasper. This 2-D sensing grasper (Fig. 3-b2)) enhanced the resolution of the pulling force by 43 mN and the grasping force by 7.4 mN [103]. Similarly, Yu et al. integrated double E-type beams with four strain gauges into the grasper jaws (Fig. 3-b3)) and achieved 3-D force decoupling measurement with a high resolution of 10 mN. However, the width of 11.2 mm exceeded instrument size limitations for laparoscopic surgery [70, 104]. Moreover, Hou et al. developed a miniature 3-D sensing chip with highly integrated four piezoresistive membranes that can be easily

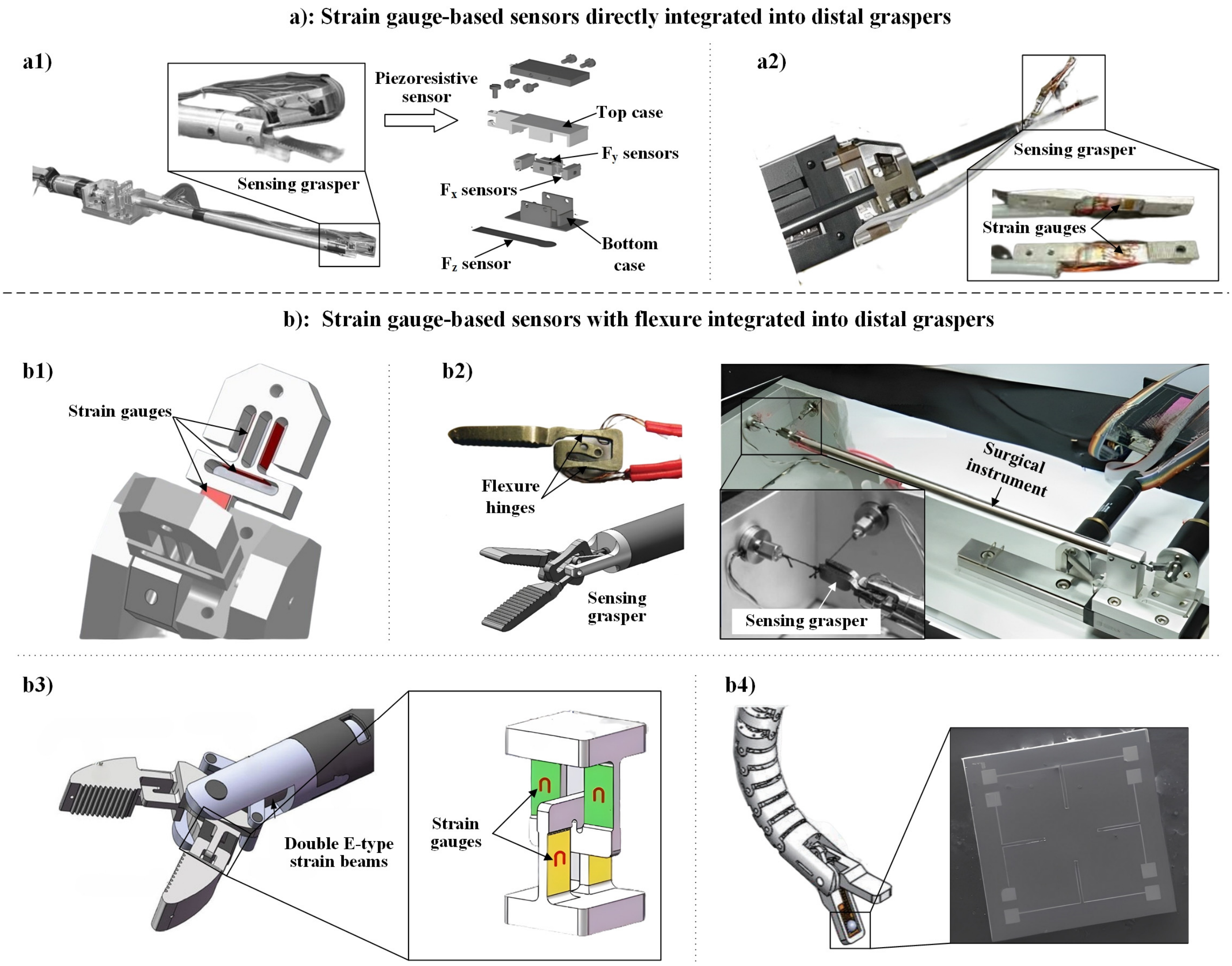

Fig. 3. Strain gauge-based force sensors that are integrated into the distal graspers of laparoscopic instruments. a1) Piezoresistive sensor integrated into the jaw back for 3-D grasping force measurement [100], © 2004 Springer; a2) Sensing grasper with two sets of strain gauges for measuring axial and bending forces [101], © 2006 IEEE; b1) 3-D sensing grasper with planar elastic beams in three orthogonal directions [102], © 2010 IEEE; b2) The proximal 2-D grasping force sensor based on flexure hinges [103], © 2012 IEEE; b3) The proximal 3-D grasping force sensor based on double E-type strain beams [70], © 2018 IEEE; b4) Miniature 3-D sensing chip assembled into the grasper [105], © 2021 IEEE. All figures are reprinted with permission of the corresponding references.

assembled into the grasper (Fig. 3-b4)). This sensor reached linearity measurement of the radial forces within [0, 0.5 N] and axial force within [0, 2 N], but its drawback of crosstalk was noticeable due to fabrication errors [105].

In addition, it is commonly challenging for strain gauge-based sensors to withstand sterilization cycles, preventing their practical applications in the clinic. Trejos et al. developed a sterilizable 3-D sensing laparoscopic grasper by selecting a particular combination of adhesives and coatings, ensuring the strain gauges maintain their functions after up to six sterilization cycles [37, 106].

Strain gauge-based sensors are widely utilized in engineering and related academic research for their high accuracy, small size, high reliability, support for multi-axial force sensing, and cost-effectiveness. However, this type of sensor still needs to overcome the sensitivity to EMI and integration difficulties due to external wires and complex circuits. The performance of strain gauge-based sensors for laparoscopic instruments is summarized in Table II.

C. Capacitive-based Force Sensing

Capacitive-based force sensors typically utilize sandwich-shaped structures with two parallel electrode plates separated by dielectrics, which enables convenient 1-D distributed force measurement within a small thickness [49, 107]. In 1994, Howe et al. first introduced a self-developed capacitive sensor and attached it to the distal end of laparoscopic instruments for exploring and localizing hidden arteries and tumors during MIS procedures. This sensor utilized two sets of crossed copper strips as electrodes and thin middle strips of silicone rubber as the dielectric substance to develop a tactile sensor (Fig. 4-a1)), achieving 1-D pressure distribution measurement within [0, 2 N]. However, as a preliminary exploration, further research was required on minimization, signal processing, and sensor integration [107-109]. Based on the microelectromechanical systems (MEMS), Paydar et al. proposed a miniaturized thin-film capacitive force sensor that was compatible with the Da Vinci Cadiere graspers. This sensor consisted of 2×3 sensing elements, and each element utilized a spring-like middle

TABLE II
SUMMARY OF STRAIN GAUGE-BASED FORCE SENSORS FOR LAPAROSCOPIC SURGERY

Authors	Year	Integrated Location	Sensing DoFs	Experiments	Range	Sensitivity	Resolution	Characteristics	Size
Bicchi et al. [72, 73]	1996	Instrument shaft	1	Model	N/A	N/A	N/A	N/A	21.3 mm×61.4 mm
Hu et al. [95]	2002	Driving unit	1	Model	N/A	N/A	N/A	N/A	N/A
Brown et al. [96, 97]	2003	Driving unit	1	In-vivo	N/A	N/A	N/A	N/A	N/A
Prasad et al. [74]	2003	Instrument shaft	2	In-vivo	0-12 N	N/A	N/A	Error: F_x: 4.9%; F_y: 3.7%.	ϕ10 mm×358.9 mm
Shimachi et al. [84]	2003	Instrument shaft and driving unit	3	Model	±10 N	N/A	0.05 N	Absolute accuracy: 0.3 N	N/A
Seibold et al. [88-91]	2004	Instrument shaft	6	Calibration	Force: ±2.5 N Torque: ±80 N·mm	N/A	F_x, F_y: 0.05 N F_z: 0.25 N	N/A	ϕ10mm
Shimachi et al. [81, 82]	2004	Instrument shaft and driving unit	3	Calibration	±10 N	N/A	0.02 N	Absolute accuracy: 0.05-0.1 N Linearity error: 5%	N/A
Tholey et al. [99, 100]	2004	Grasper	3	Model	0-1 N	N/A	N/A	Hystrersis: <0.1 N	0.6×1.75×0.5 inch^3
Mayer et al. [75]	2006	Instrument shaft	2	Model	N/A	N/A	N/A	N/A	N/A
Tholey et al. [76, 77]	2007	Instrument shaft and grasper	3	Model	F_g: 0-13 N F_i: 0-10 N	N/A	< 0.1 N	N/A	N/A
Shimachi et al. [83]	2008	Instrument shaft and driving unit	3	Calibration	±10 N	F_z: 1.5 μm/N F_x, F_y: 40 μm/N	5 mN	Error: F_x, F_y: 0.1 N Total: 0.5 N	N/A
Trejos et al. [80]	2009	Instrument shaft	5	Calibration	F_a: 0-50 N F_i: ±5 N Torque: ±80 N·mm F_{axial}: ±25 N	F_a: -0.0022 V/g F_i: -0.0295 V/g Torque: -0.0051 V/g F_{axial}: -0.00051 V/g	N/A	RMSE: F_a: 0.35 N F_i: 0.07 / 0.03 N Torque: 1.5 N·mm	N/A
Stephan et al. [102]	2010	Grasper	4	Calibration	0-10 N	N/A	0.1 N	RMS noises: F_x: 0.13 N, F_y: 0.20 N F_z: 0.05 N	8 mm×10 mm
Hong et al. [103]	2012	Grasper	2	Calibration	±5 N	N/A	F_p: 43mN F_g: 7.4 mN	RMSE: F_p: 95 mN, F_g: 37 mN Hysteresis: F_p: 1.06%, F_g: 1.53%.	N/A
Dalvand et al. [78, 79]	2013	Instrument shaft and driving unit	3	Model	F_g: 0-5 N F_i: 0-2 N	N/A	N/A	Error: F_i< 0.05 N	7.4 mm×3.3 mm
Jiang et al. [85-87]	2013	Instrument shaft	6	Ex-vivo	Force: 10 N Torque: 150 N·mm	N/A	N/A	Coupling errors: <4.29%	ϕ9.8 mm×6 mm
Trejos et al. [37]	2014	Instrument shaft	3	Calibration	F_i: ±5 N F_g: 0-17 N	N/A	N/A	Accuracy: 0.15-1.70 N Hystrersis: 0.11-1.05 N	N/A
He et al. [63]	2014	Driving unit	4	Suturing experiment	0-200 N	0.0257 V/N	40 mN	Accuracy: 0.4 N	ϕ10 mm×12 mm

(Continued)

TABLE II
(Continued) SUMMARY OF STRAIN GAUGE-BASED FORCE SENSORS FOR LAPAROSCOPIC SURGERY

Authors	Year	Integrated Location	Sensing DoFs	Experiments	Range	Sensitivity	Resolution	Characteristics	Size
Li et al. [36]	2015	Instrument shaft	3	Ex-vivo	F_{axial}: ±3.0 N F_{radial}: ±1.5 N	N/A	F_{radial}:0.015 N F_{axial}: 0.15 N	Hysteresis: <2.1% RMS error: 1.8% Max frequency: 1.25 Hz	ϕ10 mm×30 mm
Li et al. [67, 92]	2015	Instrument shaft	6	Ex-vivo	Force: ±10 N Torque: ±160 N·mm	N/A	F_x, F_y: 0.12 N F_z: 0.5 N M_x, M_y, M_z: 6.72 N·mm	Hysteresis: 2.5% RMSE: 2.0%	ϕ10 mm
Matich et al. [98]	2016	Driving unit	1	Calibration	0-40 N	2 mN/count	N/A	Linearity error: 0.16 N Hysteresis: 0.1 N	N/A
Matich et al. [93, 94]	2017	Instrument shaft	6	Calibration	F_x, F_y: ±4 N F_z: ±1 N M_x, M_y: ±60 mNm M_z: ±35 mNm	N/A	N/A	Linearity error: <0.97% Hysteresis error: <1.16% Cross error: <2.76%	ϕ9 mm
Yu et al. [70, 104]	2018	Grasper	3	Calibration	±2.5 N	N/A	0.01 N	Accuracy: F_g: 23 mN F_s: 2.2 mN F_r: 93 mN	36.15 mm×11.2 mm×7 mm
Hou et al. [105]	2021	Grasper	3	Model	F_x, F_y: 0-0.5 N F_z: 0-2.0 N	N/A	N/A	N/A	2 mm×2 mm×0.4 mm

F_I-Instrument force; F_g-Grasping force; F_p-Pulling force; F_s-Radial shear force; F_r-Axial tangential force; F_a-Actuation force; RMSE-Root mean square error.

dielectric positioned between two metal plates. Calibration experiments demonstrated that this sensor realized the measurement range of [0, 40 N] but with low linearity [110]. Moreover, Peng et al. presented a capacitive sensor composed of 5×5 sensing elements, and each element consisted of two electrodes separated by an air gap and an insulation layer, as shown in Fig. 4-a2). These elements possessed two different stiffness values and were arranged alternately, which produced distinct capacitance variations in response to pressure and thereby enabled the elasticity measurement of target objects [111]. However, these early laboratory-developed sensors encountered limitations in terms of low linearity, limited measurement range or resolution, and complex integration.

To further enhance measurement performance, commercial capacitive sensor arrays have been developed and employed for laparoscopic instruments. Ottermo et al. attached a commercial capacitive sensor pad (TactArray, Pressure Profile System, US) with 4×15 sensor elements onto a laparoscopic grasper [112], as shown in Fig. 4-a3). Trejos et al. further integrated the advanced commercial tactile sensor from the same company into the laparoscopic palpation probe and then mounted them on a robotic arm (Fig. 4-a4)). The ex-vivo experiments [113, 114] were performed with augmented hybrid impedance control, demonstrating a 50% increase in tumor detection accuracy with palpation force reduced by 35%. Furthermore, this group also developed a self-made, economical, and disposable capacitive sensor with a sandwiched compressible dielectric elastomer. This sensor provided kinesthetic feedback within [25, 150 kPa] with a resolution of 1 kPa; however, the spatial resolution of 2 mm×2 mm was limited by the size of the sensing elements [115, 116].

Although these sensors were capable of 1-D distributed force sensing and convenient for palpation, they were unsuitable for integration into complex surgical tools such as graspers. The integration process resulted in a smooth jaw surface, compromising the grasping capacity, and leading to instability during operation [112]. Moreover, multidimensional capacitive sensors faced the challenge of significant crosstalk and parasitic capacitance. Therefore, the design and integration of multidimensional capacitive-based sensors typically required modifications on the original laparoscopic graspers to achieve miniaturization without compromising their original function [47, 48].

Lee et al. presented a preliminary design of a 3-D capacitive force sensor consisting of 3 different pairs of electrodes with one shared dielectric substrate (Fig. 4-b1)) in 2013. Three electrode pairs were designed with different shapes to facilitate the low crosstalk measurement of the normal force and shear forces. Two fabricated sensors were integrated between the surgical graspers' base plate and the tooth plate, achieving a measurement range of [0, 11.7 N] but with low sensitivity due to the interference capacitance and assembly error [47]. Dai et al. proposed a 3-D force sensor (Fig. 4-b2)) that could be conveniently installed into commercial robotic laparoscopic graspers. This sensor comprised a top layer with 6 electrodes, a middle dielectric layer, and a bottom electrode layer, and thus formed six capacitive sensing cells. These capacitive cells were

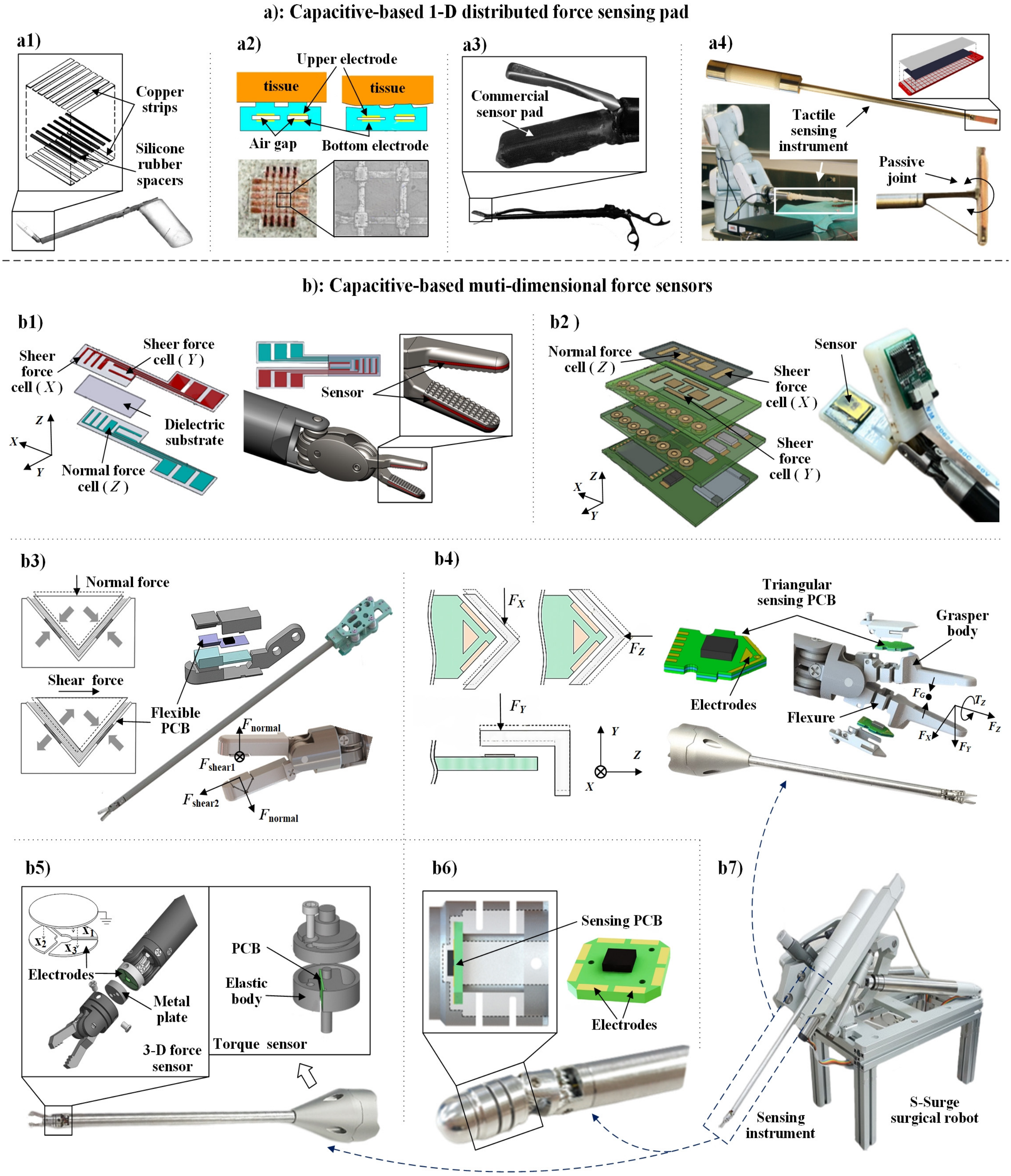

Fig. 4. Development of capacitive-based force sensors for laparoscopic surgery. a1) Sensing pad with 8*8 sensing element [109], © 1998 ASME; a2) Sensing pad with 5*5 sensing elements with two stiffness values [111], © 2009 IEEE; a3) Commercial sensing pad covered on the grasper [112], © 2006 Lippincott Williams & Wilkins; a4) Commercial sensing pad integrated into a palpation probe [133], © 2009 SAGE Publications; b1) 3-D force sensor embedded into the grasper [47], © 2013 IEEE; b2) 3-D force sensor with 6 symmetrically distributed sensing cells [117], © 2017 IEEE; b3) 2-D force sensor based on a triangular prism [121], © 2015 IEEE; b4) 3-D force sensor based on a triangular-shaped sensing PCB and a grooved flexure [69, 123], © 2016 IEEE, © 2019 IEEE; b5) Sensing instrument with a 3-D distal force sensor and two proximal torque sensor [119, 124], © 2015 IEEE, © 2017 IEEE; b6) 6-D F/T sensor for palpation probe [126], © 2018 IEEE; b7) S-Surge surgical robot with different sensing instruments [124], © 2017 IEEE. All figures are reprinted with permission of the corresponding references.

divided into three pairs for measuring the normal force and two shear forces, respectively. Each pair was symmetrically distributed on the sensing PCB to create differential capacitance, thus reducing errors caused by crosstalk and parasitic capacitance as well as improving the accuracy and signal-to-noise ratio of this sensor. However, the large sensor size of 11 mm×15 mm×0.6 mm with complex circuitry and the absence of grasper tooths made it challenging to apply in laparoscopic surgery [117, 118]. Additionally, the radial force measurement of the above two sensors was realized based on the overlap area variation of the two electrodes. This type of sensor typically necessitates a complex structure and is highly susceptible to manufacturing error and parasitic capacitance.

According to the principle of capacitive sensing, sensors based on overlap area change can achieve better linearity. However, the accuracy of this sensor type is highly susceptible to manufacturing and assembly errors, and multidimensional force sensors are more prone to generate severe crosstalk. As a result, the group at Sungkyunkwan University adopted the distance variation principle to develop highly integrated multidimensional capacitive sensors [48, 119]. These sensors reached a better resolution with a miniature size that can be easily integrated into the distal end of laparoscopic instruments.

Kim et al. proposed a 2-D miniaturized capacitive-based force sensor consisting of a triangular prism with two sensing cells to measure the normal and shear forces (Fig. 4-b3)). The capacitive response of both sensing cells exhibited identical changes under normal force, whereas they produced different changes under the shear force. Two proposed sensors were orthogonally integrated into the two jaws of laparoscopic instruments to measure the 3-D operation forces and the grasping force [120, 121]. Moreover, this group developed a 3-D force sensor consisting of a triangular-shaped sensing PCB with three electrodes and a grasper body with an embedded flexure to improve the sensitivity, as illustrated in Fig. 4-b4). The air gaps between them formed three orthogonal capacitive sensing units to measure F_x, F_y, and F_z, respectively. This sensor achieved satisfactory resolution values of 3.8 mN, 1.8 mN, and 2.0 mN within [-5 N, 5 N] for F_x, F_y, and F_z, respectively. Two proposed sensors were integrated into the proximal region of two jaws to measure the 5-D F/T and supported palpation at the backside or edge of the grasper. Ex-vivo experiments with electro-cautery tasks were conducted utilizing the surgical robot S-Surge (Fig. 4-b7)) equipped with this sensing grasper [48, 69, 122, 123]. Both highly integrated sensor designs enabled direct measurement of interaction forces and torque. However, the former design lost the functional surface of the surgical instrument, while the latter led to an increase in the graspers' size.

To preserve the grasper's original function and shape, Lee et al. designed a 3-D distal force sensor integrated into the wrist to measure instrument forces and developed another 1-D torque sensor integrated into the proximal driving unit to indirectly estimate grasping force (Fig. 4-b5)). The force sensor comprised three fan-shaped electrodes and one circular electrode, forming three sensing units and achieving the 3-D force measurement. Similarly, the proximal torque sensor estimated the distal grasping force by measuring the distance variation between the PCB's electrode and the elastic metal body, which is generated by the cable tension. However, their linear measuring ranges were restricted to [0, 50N·mm], [0, 1 N], [0, 1 N], and [0, 1.6 N], respectively [66, 119, 124, 125]. Furthermore, Kim et al. developed a sensing probe by installing a miniature 6-D capacitive sensor with 8 sensing cells. These sensing cells were composed of 8 positive electrodes integrated into the edges of a sensing PCB, a shared negative electrode based on a deformable flexure, and the dielectric involved 8 parallel and orthogonal air gaps sandwiched between the electrodes (Fig. 4-b6)). The capacitance values of the 8 sensing cells exhibited different variations under 6-D F/T, which theoretically avoided crosstalk. Ex-vivo experiments were conducted using the S-Surge robot equipped with this sensing instrument, demonstrating its ability to accurately identify organizations with different stiffness values and cancerous regions [126].

Overall, the capacitive-based sensors offer several benefits, including simple and compact structure, low cost, high sensitivity, and insusceptibility to environmental factors such as temperature, humidity, and magnetic field, making them suitable for the complex environment of RALS. However, this type of sensor suffers from a limited measurement range, poses challenges for multi-axial force measurement due to the crosstalk and parasitic capacitance, as well as requires excellent packaging and high-precision manufacturing to guarantee accuracy and reliability. The performance summary of capacitive-based sensors for laparoscopic instruments is listed in Table III.

D. Optical Fiber-based Force Sensing

Optical fiber-based sensors have attracted a surge of attention for force sensing on RALS [7, 127-129], owing to the superior advantages such as miniature size, excellent sensitivity, insensitivity to EMI, strong corrosion resistance, satisfied biocompatibility, etc. The optical fiber-based force sensing techniques for RALS mainly employ three types: LIM-based, wavelength modulation-based, and phase modulation-based [130, 131]. The phase modulation-based sensors were typically utilized for the 1-D force measurement at the tip of surgical needles. These implementations commonly require the solid central part to carry the reflective mirror, making it challenging to pass driving wires in the instrument shaft, and limiting their practical applications [57, 58, 132, 133]. Therefore, this section will focus on LIM-based force sensors and FBG-based force sensors.

1) **LIM-based Force Sensing**

Peirs et al. introduced the first FOS for RALS in 2004. They employed a sensing flexure with four identical parallelograms that exhibited distinct deformations under axial and radial forces, enabling the 3-D force measurement (Fig. 5-a)). Three optical fibers were arranged at 120° intervals in the proximal part, and their shared reflective surface was attached to the distal part to measure the force-induced deformation of the flexure through the reflected light intensity. This sensor was integrated into the wrist of a laparoscopic instrument and

TABLE III
SUMMARY OF CAPACITIVE-BASED FORCE SENSORS FOR LAPAROSCOPIC SURGERY

Authors	Year	Integrated Location	Sensing DoFs	Experiments	Range	Sensitivity	Resolution	Characteristics	Size
Howe et al. [107-109]	1994	Palpation probe	1	Model	0-2 N	N/A	N/A	Noise level: <1 mN Max frequency: 16 Hz	20 mm×20 mm
Ottermo et al. [112]	2006	Palpation probe	1	Ex-vivo	0-0.7 MPa	N/A	N/A	Localization resolution: 2 mm	30 mm×8 mm
Peng et al. [111]	2009	N/A	1	Calibration	0.1-0.5 MPa	N/A	0.1 MPa (5 mN)	N/A	10.2 mm×10.2 mm
Trejos et al. [113, 114]	2009	Palpation probe	1	Ex-vivo	0-14 MPa	N/A	N/A	N/A	35 mm×10 mm
Payder et al. [110]	2012	N/A	1	Calibration	0-40 N	N/A	N/A	Min. error: 2.1% Max frequency: 20 kHz	1 mm^2 and 9 mm^2
Lee et al. [47]	2013	Grasper	3	Calibration	0-11.7 N	F_x: 11.6 fF/N F_y: 10.8 fF/N F_z: 7.5 fF/N	N/A	N/A	13 mm×5 mm
Naidu et al. [115, 116]	2016	Palpation probe	1	Ex-vivo	25-150 kPa	N/A	1 kPa	Localization resolution: 2 mm Max frequency: 30 Hz	49 mm×10 mm×2.5 mm / 30 mm×8 mm×2.5 mm
Kim et al. [120, 121]	2016	Grasper	4	Model	F_x: ±2.5 N F_y: ±5 N F_z: ±2.5 N F_g: 5 N	N/A	F_x: 42 mN F_y: 58 mN F_z: 72 mN F_g: 46 mN	RMS error: F_x: 1.23%, F_y: 1.58%, F_z: 1.34%, F_g: 1.56% Hysteresis: F_x: 1.96%, F_y: 2.16%, F_z: 2.03%, F_g: 1.75%	N/A
Dai et al. [117, 118]	2017	Grasper	3	Model	0-12 N	F_x: 0.598 fF/N F_y: 1.038 fF/N F_z: 25.3 fF/N	F_x: 268 mN F_y: 127 mN F_z: 4 mN	Max frequency: 109 Hz	11 mm×15 mm×0.6 mm
Kim et al. [48, 69, 122, 123]	2018	Grasper	5	Ex-vivo	±5 N	N/A	F_x: 3.8 mN F_y: 1.8 mN F_z: 2.0 mN	Relative error: F_x: 2.6%, F_y: 2.2 %, F_z: 1.3% Max frequency: 430 Hz	N/A
Kim et al. [126]	2018	Instrument shaft	6	Ex-vivo	Forces: ±1.0 N Torque: T_x, T_y: ±20 N·mm T_z: ±10 N·mm	N/A	Forces: 0.21 mN Torque: 0.35 N·mm	Relative error: Force:5.5% Torque: 2.7% Hysteresis: 1.52% Max frequency: 434 Hz	ϕ10 mm×10 mm
Lee et al. [66, 119, 124, 125]	2020	Instrument shaft	4	Model	F_x: 1 N F_y: 1 N F_z: 1.6 N Torque: 50 N·mm	N/A	N/A	Hysteresis: F_x: 2.6%, F_y: 2.2%, F_z: 1.3%, Torque: 1.6%	Force sensor: ϕ8 mm×17 mm Torque sensor: ϕ16 mm×10 mm

F_g-Grasping force.

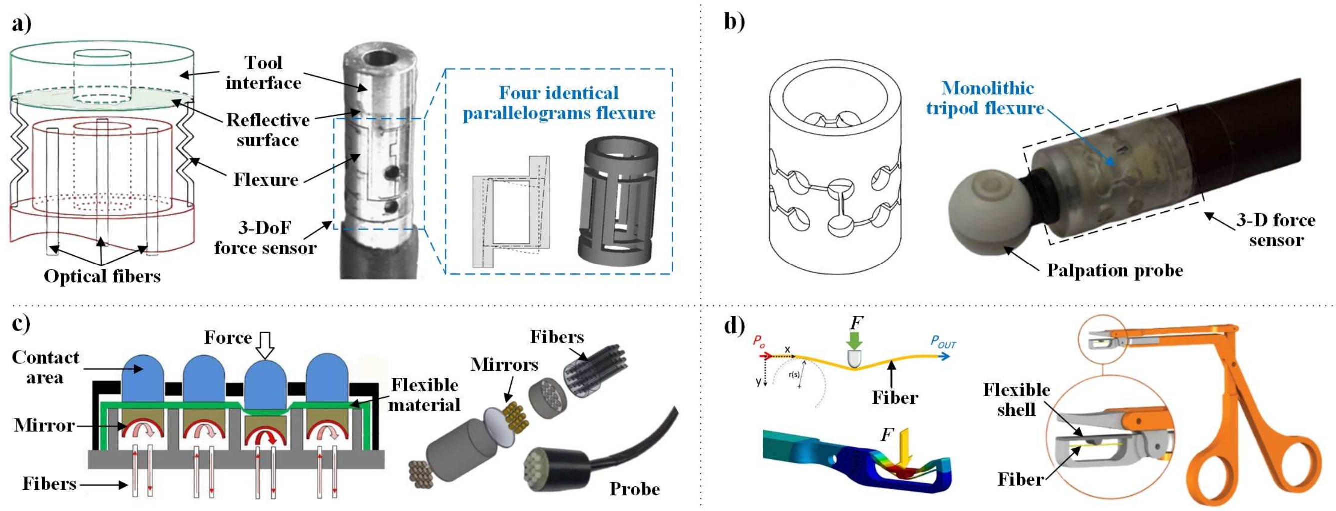

Fig. 5. Development of LIM-based force sensors for laparoscopic surgery. a) 3-D force sensor based on four identical parallelograms flexure [134], © 2004 Elsevier; b) 3-D force sensor based on monolithic tripod flexure [135], © 2012 IEEE; c) Sensing probe with 14 elements [136], © 2014 IEEE; d) Grasping force sensor integrated into a jaw [56], © 2020 IEEE. All figures are reprinted with permission of the corresponding references.

achieved the measurement ranges of [0, 2.5 N] for axial force and [0, 1.7 N] for radial forces, but the manufacturing error limited its resolution to 40 mN [134]. Puangmali et al. adopted the same fiber configuration to achieve the 3-D force measurement and additionally integrated a reference fiber to compensate for optical signal variations resulting from fiber bending, intensity drifts, and environmental temperature (Fig. 5-b)). A monolithic flexible tripod structure as the sensing structure was arranged symmetrically around the central axis of the instrument, providing axial flexibility while maintaining torsional and lateral stiffness. Benefiting from the improved flexible structure, this sensor achieved a resolution of 20 mN at an axial force range of ±3 N and a radial force range of ±1.5 N [135]. Furthermore, in contrast to the above-mentioned two sensors that achieve 3-D force palpation at a single point, Xie et al. proposed a probe head (Fig. 5-c)) equipped with 14 sensing elements to detect tissue abnormalities based on the force spatial distribution. Each sensing element consists of a transmitting and a receiving fiber to perceive light intensity variations and obtain the applied force information. However, the measurement range of the sensing elements was limited to [0, 0.5 N] with a resolution of 50 mN. Both phantom and ex-vivo tissue experiments validated the probe's ability to generate high-resolution stiffness maps and precisely locate the tumor [55, 136, 137].

In addition to integrating the LIM-based sensors into the wrist of the instruments, Bandari et al. developed a miniaturized LIM-based sensing grasper (Fig. 5-d)). A single-mode optical fiber was attached to a substrate located on the lower jaw of the grasper. The grasping force was applied to the optical fiber through the indenter under the substrate, bending the optical fiber and producing a power loss [56]. Besides, benefiting from the advantages of miniaturization size and high accuracy, the LIM-based sensors can also be integrated into catheter tips for 1-D or 3-D force measurement [54, 138]. The LIM-based sensors offer the advantages of simple structure, cost-effectiveness, and ease of implementation, rendering them widely utilized for measuring tool-tissue interaction force, torque, and pressure. However, the accuracy and repeatability of these devices are easily affected by variations in input light intensity and fiber bending loss [35, 139].

2) **FBG-based Force Sensing**

Müller et al. introduced the first application of FBG-based F/T sensors for robot-assisted laparoscopic instruments in 2009. Inspired by the Stewart parallel platform, this sensor utilized a thick-walled pipe structure as sensing flexure and suspended a fiber embedded with 6 FBG elements as six links around the flexure (Fig. 6-a1)). The applied F/T can induce a relative deformation between two plates, resulting in strain change on the internal linkages. By measuring the strain in these links, it is possible to calculate the 6-D F/T exerted on the sensor based on stiffness and calibration matrix [140]. Kim et al. utilized a similar approach to develop a 6-D F/T sensor, as depicted in Fig. 6-a2). They adopted a slender cylinder to connect the upper and lower platforms, improving the F/T resolution values to 15 mN and 5 N·mm, respectively [141]. Haslinger et al. devised a miniaturized and compact 6-D F/T sensor based on a parallel Stewart mechanism and attached six FBG elements on the six links with an additional FBG element for temperature compensation (Fig. 6-a3)). Moreover, the fully encapsulated design enabled this sensor to satisfy the requirements of biocompatibility and sterilizability [142]. Despite these Stewart-based sensor designs being able to easily implement 6-D F/T measurements with high stiffness and simple configuration, they have not been integrated into laparoscopic instruments for practical applications due to negative factors such as low sensitivity, non-linearity, crosstalk, or hysteresis.

Adopting different types of flexible beams and their variations as sensing flexure is a typical and essential design method of force sensors for RALS. Song et al. directly attached four FBGs to the four vertical beams that were distributed around the wrist of the laparoscopic manipulator to determine, F_z, M_x and M_y (Fig. 6-a4)). This sensor was integrated into a 7-DoF robotic manipulator and achieved a resolution of 50 mN within 10 N, but with a large maximum error of 100 mN due to the interference from driving cables [143]. However, as a result of the high axial stiffness of the instrument shaft, it is essential to separately design axial-force sensing structures with a lower stiffness value to improve the sensitivity and accuracy of F_z. Wang et al. [64] combined an axial force sensing zone with two notches perpendicular and a radial force sensing zone based on three flexible vertical beams in a serial configuration (Fig. 6-a5)). Du et al. [144, 145] employed the cross beam and four vertical flexible beams to measure axial and radial forces, respectively (Fig. 6-a6)), extending the measuring range to [0, 11 N] with a small linearity error of 0.6% and low hysteresis of 0.3%.

Furthermore, the mechanism-based approach to designing force-sensitive flexure for sensors was employed by Tianjin University, allowing sensors to achieve more comprehensive performances. The rigid body replacement method [146] was utilized to enable flexures to inherit properties of the original rigid mechanisms. Lv et al. proposed a compact 1-D force sensor composed of a miniature force-sensitive parallel structure with four flexure hinges prototyped from the Sarrus mechanism (Fig. 6-a7)). This design achieved an excellent axial force resolution of 2.55 mN with a low crosstalk error of 2.3%, owing to its unique 1-DoF configuration along the *z* axial [65]. To enhance the measurement range, this group [147] developed another 1-D distal force sensor consisting of 6 miniature and parallel flexural links and two plates to replace the rigid Stewart platform (Fig. 6-a8)), inheriting the robust load capability of the original mechanism and achieving an extensive measurement range of [0, 12N]. Two miniature FBG-enabled torque sensors for MIS robots have also been developed with specially designed torque-sensitive flexure based on this principle and achieve high sensitivity values [148, 149]. These merits have been extended to design force-sensitive or force-displacement flexures for FBG-based wearable or handheld sensors to monitor physiological signals [150-152]. Furthermore, utilizing the freedom and constraint topology (FACT) method, Tang et al. proposed a 3-D force sensor with an axial and radial force-sensitive structure in a serial connection [35]. The axial force-sensing structure adopted a double-layer cross-beam, while the radial force-sensing structure comprised four spatial linkages along the edge direction of a spatial tetrahedral (Fig. 6-a9)). This sensor theoretically eliminated the crosstalk between axial and radial forces, with simulation indicating a maximum crosstalk of 2.24%. Experimental results demonstrated excellent resolution values of 1.18 mN and 1.81 mN in F_x, F_y within [-5 N, 5 N], and 2.61 mN in F_z within [0, 5 N].

The aforementioned sensors are specifically designed for integration into the distal end of surgical instruments' shafts to accurately measure instrument forces or perform palpation. Additionally, there exist various FBG sensors that are dedicated to directly measuring the tool–tissue interaction forces while surgeons manipulate scissors or graspers. Callaghan et al. first presented a sensing scissor by directly bonding a single FBG element at the proximal location of a tapered manual blade (Fig. 6-b1)). This sensing blade achieved a resolution of 0.5 N within [0, 30 N], supported measuring blade-tissue interaction forces, and avoided interfering with blade operational function during surgery [71, 153, 154]. Fattahi et al. utilized a similar method that mounted two FBG fibers at the outer side of the grasper jaw to measure the grasping force and employed an additional FBG element for temperature compensation (Fig. 6-b2)). However, this research was mainly conducted in simulation rather than the actual implementation [155].

Instead of directly pasting the FBG element on the scissors or graspers, the sensor sensitivity can be further enhanced by implementing flexure. Christoph et al. [156] utilized two trapezoidal structures as sensing flexures to measure the grasping and spreading forces; each flexure was equipped with a suspended FBG element (Fig. 6-b3)). Zarrin et al. proposed a sensing grasper featuring a T-shaped jaw and incorporating a parallel grooved flexure in the proximal region of the jaw (Fig. 6-b4)). Two FBG elements were arranged to the jaw's distal region and grooved flexure to measure the grasping and pulling forces, respectively [157, 158]. The grasping force and axial force measurement sensitivity of this sensor reached 15.5 pm/N within [0, 10 N] and 6 pm/N within [0, 6 N], respectively. However, it is susceptible to crosstalk from other directions, producing challenges for performing high-precision operations. Moreover, the variable grasping positions during grasping soft tissue significantly affect the accuracy of these designs. To tackle the above issues, Sun et al. [68] proposed a force-sensitive grasper with bridge-type flexure that linearly transformed and amplified the vertical force applied to the grasper surface into an axial deformation of the FBG element integrated along the flexure centerline, as illustrated in Fig. 6-b5). This sensor has been integrated into a self-made surgical grasper and exhibited excellent load-bearing capacity and anti-interference ability [159]. The calibration experiments have demonstrated similar sensitivities of 56.2 pm/N, 51.1 pm/N, and 47.5 pm/N for three different grasping positions within [0, 10 N], and both ex-vivo and in-vivo animal experiments for tissue detection and grasping have validated the efficacy of the designed sensor.

Additionally, Xue et al. employed an indirect measurement approach that integrated sensors into the driving unit to estimate the force exerted on the RALS instrument. The proposed sensor consisted of six cantilevers with cable-housed canals, and each cantilever was equipped with an FBG element attached to its groove, enabling measurement of minimal deformation caused by cable tension. The calibration experiment indicated that this sensor could measure cable tension values of up to 68.6 N with a sensitivity of 83.8 pm/N, but suffered from a relatively high linearity error due to the poor stress-strain linear relationship of the adopted Polyamide material [40].

FBG utilizes the wavelength modulation methodology, which offers the benefit of insensitivity to input light sources and fiber bending loss. The advantages of high sensitivity, excellent linearity, and support for multiple-point detection also make FBG-based sensors more promising for widespread development and application in force sensing for RALS. Consequently, FBG-based sensors are also extensively utilized in retinal microsurgery [160-163], robotic catheterization [164-170], physiological signal measurement [151, 171-173], and

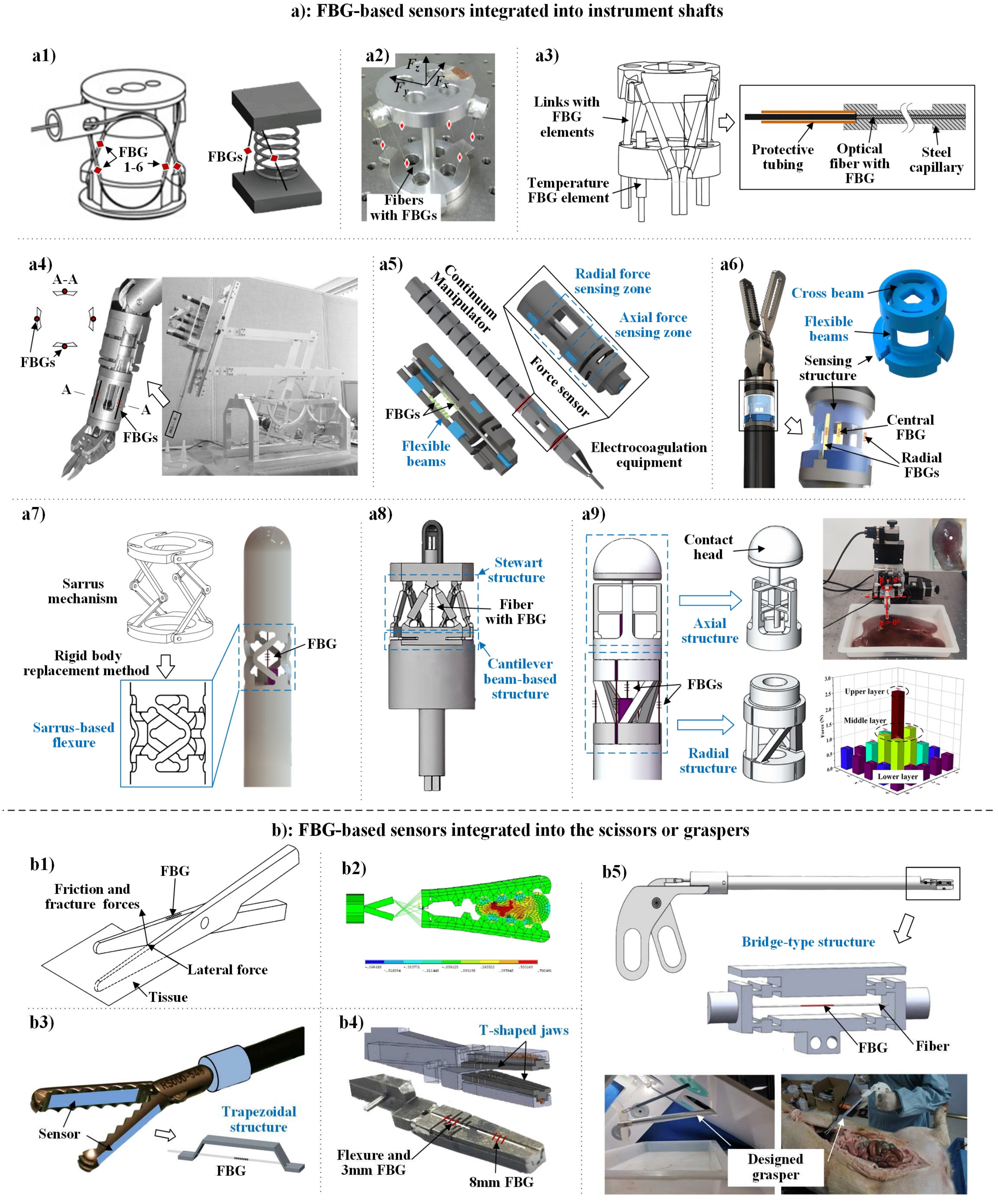

Fig. 6. Implementation of FBG-based force sensors for laparoscopic surgery. a1) 6-D F/T Stewart inspired sensor based on a thick-walled pipe structure [140], © 2009 Taylor & Francis; a2) 6-D F/T sensor utilizing a slender cylinder [141], © 2016 Springer ; a3) 6-D F/T sensor equipped with 6 fully encapsulated links [142] © 2013 IEEE; a4) Four vertical beams-based 3-D force sensor for the 7-DoF robotic manipulator [143], © 2011 American Institute of Physics; a5) 3-D force sensor based on two notches perpendicular and vertical beams [64], © 2021 IEEE; a6) 3-D force sensor based on the cross beam and four vertical flexible beams [145], © 2022 IEEE; a7) 1-D palpation sensor with Sarrus-based flexure [65] © 2019, Biomedical Engineering Society; a8) 1-D force sensor with Stewart-inspired flexure and cantilever beams [147], © 2020 IEEE; a9) 3-D force sensor developed by the FACT method [35], © 2022 IEEE; b1) Sensing manual blade [153], © 2011 IOP Publishing; b2) Simulation of a sensing grasper with FBG elements mounted at the jaw [155], © 2011 IEEE; b3) Sensing grasper based on the trapezoidal structure [156], © 2014 SPIE; b4) Sensing T-shaped jaws [158], © 2018 IEEE; b5) Sensing grasper based on the bridge-type flexure and the in-vivo experiment [68], © 2021 IEEE. All figures are reprinted with permission of the corresponding references.

TABLE IV

SUMMARY OF FBG-BASED FORCE SENSORS FOR LAPAROSCOPIC SURGERY

Authors	Year	Integrated Location	Sensing DoFs	Experiments	Range	Sensitivity	Resolution	Characteristics	Size
Müller et al. [138]	2009	N/A	6	Calibration	F_x: 0-10 N F_y: 0-10 N F_z: 0-20 N M_x: 0-20 N·cm M_y: 0-14.2 N·cm M_z: 0-9.8 N·cm	F_x: 19 pm/N F_y: 30 pm/N F_z: 42 pm/N M_x: 37 pm/Ncm M_y: 30 pm/Ncm M_z: 80 pm/Ncm	F_x: 211 mN F_y: 133 mN F_z: 95 pm/N M_x: 108 mN·cm M_y: 133 mN·cm M_z: 50 mN·cm	N/A	10 mm×10 mm×10 mm
Song et al. [141]	2011	Instrument shaft	3	Calibration	0-10 N	N/A	50 mN	Max error: 0.1 N	N/A
Callaghan et al. [70, 146, 147]	2011	Scissor	1	Model	0-30 N	N/A	0.5 N	N/A	N/A
Haslinger et al. [140]	2013	N/A	6	Calibration	F_x: ±6.879 N F_y: ±6.879 N F_z: -6.915-0 N M_x: ±59.34 N·mm M_y: ±59.34 N·mm M_z: ±49.53 N·mm	N/A	N/A	Max crosstalk: F_z: 1.8517 N M_z: 6.5657 N·mm Max frequency: 2500 Hz	ϕ6.4 mm×6.5 mm
Christoph et al. [149]	2014	Grasper	2	Calibration	0-6 N	91 pm/N	N/A	N/A	N/A
Kim et al. [139]	2016	N/A	6	Calibration	Force: 10 N Torque: 100 N·mm	Force: 66.7 pm/N Torque: 0.2 pm/Nmm	Force: 15 mN Torque: 5 N·mm	N/A	ϕ10 mm×12 mm
Zarrin et al. [150, 151]	2018	Grasper	2	Calibration	F_g: 0-10 N F_a: 0-6 N	F_g: 15.5 pm/N F_a: 6 pm/N	F_g: 64.4 mN F_a: 166.5 mN	RMS error: F_g: 0.27 N; F_a: 0.50 N Hysteresis: F_g: 0.04 N; F_a: 0.33 N Max frequency: 100 Hz	N/A
Xue et al. [38]	2018	Driving unit	1	Calibration	0-68.6 N	83.8 pm/N	140 mN	Linearity error: ±5.57%	N/A
Lv et al. [64]	2020	Instrument shaft	1	Ex-vivo	0-5 N	392.17 pm/N	2.55 mN	Linearity error: 0.97%	ϕ 5 mm×4.9 mm
Shi et al. [145]	2020	Instrument shaft	1	Calibration	0-12 N	47.06 pm/N	21 mN	Linearity error: 0.14%	ϕ20 mm×65 mm
Wang et al. [63]	2021	Instrument shaft	3	Model	0-2 N	F_x: 77.26 pm/N F_y: 81.98 pm/N F_z: 80.82 pm/N	F_x: 14.3 mN F_y: 9.7 mN F_z: 13.8 mN	Max error: 0.1667 N	ϕ10 mm×16 mm
Sun et al. [67]	2021	Grasper	1	In-vivo	0-10 N	56.2 pm/N	17.8 mN	Linearity error: 0.37%	N/A
Du et al. [142, 143]	2022	Instrument shaft	3	Ex-vivo	0-10 N	58 pm/N	17.242 mN	Linearity error: 0.61% Hysteresis: 34.986 mN Repeatability: 62.901 mN Static error: 94.539 mN	N/A
Tang et al. [34]	2022	Instrument shaft	3	Ex-vivo	F_x: ±5 N F_y: ±5 N F_z: 0-5 N	F_x: 846.33 pm/N F_y: 553.95 pm/N F_z: 383.79 pm/N	F_x: 1.18 mN F_y: 1.81 mN F_z: 2.61 mN	Max linearity error: 1.55%	ϕ10 mm×29.5 mm

F_g-Grasping force; F_a-Axial force.

other medical applications [62, 131, 174]. These applications are not the focus of this paper and will not be discussed further. Nevertheless, the FBG-based sensors, especially for muti-dimensional measurement, require a substantial investment for the optical spectrum interrogator with multiple channels. The performance summary of various FBG-based sensors is listed in Table IV.

III. Conclusion and Outlook

This review summarizes the early research, starting implementations, and recent advances and applications in force-sensing techniques for RALS. Force-sensing techniques are indispensable for laparoscopic surgical robots to improve surgery quality, mitigate tissue damage from excessive operating forces, and facilitate training for novice surgeons [27]. Despite considerable advances and achievements in implementing various force sensors, it remains challenging to miniature sensor size, achieve multidimensional force decoupling measurements, and integrate sensors well into surgical instruments for RALS with high accuracy, measurement stability, excellent biocompatibility, and packaging [175]. Until now, there are almost no commercially available miniature force sensors to achieve robust integration with surgical instruments and support further seamless integration into the current clinical workflows [15]. To address the current issues and fulfill the specific design requirements of the force sensors for RALS, the future design can incorporate the following three essential factors: the sensing element, the integration position, and the force-sensitive structure.

For sensing element selection: The force sensors for RALS typically utilize strain gauge-based, capacitive-based, and optical fiber-based principles. Although various sensing principles and their trials on different integration positions have benefits and drawbacks, FOS represented by FBG-based sensors are more advantageous in developing highly integrated RALS instruments regarding miniature si

ze, excellent sensitivity, high biocompatibility, absence of electrical connection, and insensitivity to EMI and corrosion [60]. Furthermore, the average cost of the FBG interrogator will be significantly reduced with the possible usage of FBG-based sensors in bulk production.

For integration position determination: Various developed sensors have been integrated into the driving unit, the instrument shaft, and the end effector. Sensors located closer to the distal end of surgical instruments are typically subject to less friction, inertial forces, and F/T amplification and are easier to achieve high accuracy [7]. Despite this type of sensor suffering from the strictest requirements of miniaturization, sterilization, and packaging, integrating miniature sensors into the wrist or end-effector is more promising for achieving direct measurement of interaction forces with desirable accuracy. The temperature compensation and packaging methods are also developed to satisfy biocompatibility requirements and withstand sterilization cycles [106, 142].

For force-sensitive structure design: It is worth noting that the force-sensing structure is another crucial part but is easily ignored, apart from the sensing element and the integration position. The grooved structure is a straightforward way to reduce stiffness and improve sensitivity [126]; however, such structures are highly susceptible to significant crosstalk in multidimensional force sensors. The combination of vertical and horizontal beams, especially for Maltese cross beams, is widely adopted in multidimensional sensor design, and their corresponding crosstalk-resistant methods have been extensively developed [145]. Nevertheless, such sensing structures are usually complicated and unsuitable for installation at the distal end of miniature and highly integrated instruments for RALS. Subsequently, force-sensitive structure design from the mechanism perspective is adopted for expecting superior sensor performance. The rigid-body replacement method utilizes flexible hinges to replace the original rigid joints from advanced mechanisms, such as parallel mechanisms, forming miniature force-sensitive flexures [146]. FACT is a mechanical design framework offering a vector spaces library with visual representations to guide the analysis and synthesis of flexible systems. This method facilitates designers to quickly and accurately obtain the configuration of the force-sensitive structures based on desired DoF requirements [35]. Furthermore, topology optimization can be applied as a practical design methodology that aids designers in obtaining novel force-sensitive structures with specific functions by seeking the optimal topology or material connection from the initial structure [176]. From the mechanism perspective, the force-sensitive flexure design method has the potential to miniature sensor design and improve sensor performances, including resolution, decoupling multidimensional measurement, and anti-interference capability [177, 178]. Combining this method with the selection of the FBG sensing element can probably provide part of the framework and general guidelines or solutions for multi-axial miniature force sensor designs for RALS.

In summary, the selection of sensing elements depends on the currently available sensing principles based on physical, chemical, and even biological phenomena [42]. With the development of fundamental research, the discovery and breakthrough of these sensing phenomena can make outstanding contributions to improve sensor performances in terms of measurement sensitivity and range, biocompatibility, and miniaturization. The force-sensitive structure design from the mechanism perspective facilitates sensor miniaturization, enables multidimensional force decoupling, and enhances sensor performance indexes, including improved sensitivity, exceptional linearity, depressed crosstalk, and increased measurement range [35]. Moreover, MEMS-based sensors typically comprise microelectronic components responsible for sensing and data processing, as well as minimum mechanical components providing physical feedback, featuring excellent prospects in miniature sensors owing to their small size, low power consumption, ease of integration, and batch fabrication [179]. The existing novel manufacturing techniques, such as high-resolution additive manufacturing and laser machining, can effectively fabricate miniature and compact force-sensing flexures with different materials [180]. Consequently, these techniques support convenient sensor fabrication and integration at the distal part of the highly integrated instrument. More miniature force sensors with high performances could be developed to realize seamless and effective integration into the surgical instruments, support sophisticated operations for even microsurgery, and further enable improved and new clinical workflows.

REFERENCES

[1] V. Vitiello, S. L. Lee, T. P. Cundy, and G. Z. Yang, "Emerging robotic platforms for minimally invasive surgery," *IEEE Rev. Biomed. Eng.,* vol. 6, pp. 111-26, Mar. 2013.

[2] C. Bergeles, and G. Z. Yang, "From passive tool holders to microsurgeons: safer, smaller, smarter surgical robots," *IEEE Trans. Biomed. Eng.,* vol. 61, no. 5, pp. 1565-76, May 2014.

[3] P. E. Dupont, B. J. Nelson, M. Goldfarb, B. Hannaford, A. Menciassi, M. K. O'Malley, N. Simaan, P. Valdastri, and G. Z. Yang, "A decade retrospective of medical robotics research from 2010 to 2020," *Sci. Rob.,* vol. 6, no. 60, pp. eabi8017, Nov. 2021.

[4] H. Muaddi, M. E. Hafid, W. J. Choi, E. Lillie, C. de Mestral, A. Nathens, T. A. Stukel, and P. J. Karanicolas, "Clinical Outcomes of Robotic Surgery Compared to Conventional Surgical Approaches (Laparoscopic or Open): A Systematic Overview of Reviews," *Ann. Surg.,* vol. 273, no. 3, pp. 467-473, Mar. 2021.

[5] J. Li, S. Wang, Z. Zhang, and C. Shi, "A Robotic System for Transanal Endoscopic Microsurgery: Design, Dexterity Optimization, and Prototyping," *IEEE Robot. Automat. Mag.*, pp. 2-16, Nov. 2024.

[6] G. G. Muscolo, and P. Fiorini, "Force–Torque Sensors for Minimally Invasive Surgery Robotic Tools: An Overview," *IEEE Trans. Med. Robot. Bionics,* vol. 5, no. 3, pp. 458-471, Aug. 2023.

[7] P. Puangmali, K. Althoefer, L. D. Seneviratne, D. Murphy, and P. Dasgupta, "State-of-the-Art in Force and Tactile Sensing for Minimally Invasive Surgery," *IEEE Sensors J.,* vol. 8, no. 4, pp. 371-381, Feb. 2008.

[8] W. Zhang, H. Li, L. Cui, H. Li, X. Zhang, S. Fang, and Q. Zhang, "Research progress and development trend of surgical robot and surgical instrument arm," *Int. J. Med. Robot.,* vol. 17, no. 5, pp. e2309, Oct. 2021.

[9] C. H. Kuo, J. S. Dai, and P. Dasgupta, "Kinematic design considerations for minimally invasive surgical robots: an overview," *Int. J. Med. Robot,* vol. 8, no. 2, pp. 127-45, June 2012.

[10] O. M. Omisore, S. Han, J. Xiong, H. Li, Z. Li, and L. Wang, "A Review on Flexible Robotic Systems for Minimally Invasive Surgery," *IEEE Trans. Syst. Man Cybern.,* vol. 52, no. 1, pp. 631-644, Jan. 2022.

[11] C. Shi, X. Luo, P. Qi, T. Li, S. Song, Z. Najdovski, T. Fukuda, and H. Ren, "Shape Sensing Techniques for Continuum Robots in Minimally Invasive Surgery: A Survey," *IEEE Trans. Biomed. Eng.,* vol. 64, no. 8, pp. 1665-1678, Aug. 2017.

[12] B. S. Peters, P. R. Armijo, C. Krause, S. A. Choudhury, and D. Oleynikov, "Review of emerging surgical robotic technology," *Surg. Endosc.,* vol. 32, no. 4, pp. 1636-1655, Apr. 2018.

[13] C. D'Ettorre, A. Mariani, A. Stilli, F. Rodriguez y Baena, P. Valdastri, A. Deguet, P. Kazanzides, R. H. Taylor, G. S. Fischer, S. P. DiMaio, A. Menciassi, and D. Stoyanov, "Accelerating Surgical Robotics Research: A Review of 10 Years With the da Vinci Research Kit," *IEEE Robot. Automat. Mag.,* vol. 28, no. 4, pp. 56-78, Dec. 2021.

[14] J. Konstantinova, A. Jiang, K. Althoefer, P. Dasgupta, and T. Nanayakkara, "Implementation of Tactile Sensing for Palpation in Robot-Assisted Minimally Invasive Surgery: A Review," *IEEE Sensors J.,* vol. 14, no. 8, pp. 2490-2501, June 2014.

[15] R. V. Patel, S. F. Atashzar, and M. Tavakoli, "Haptic Feedback and Force-Based Teleoperation in Surgical Robotics," *Proc. IEEE,* vol. 110, no. 7, pp. 1012-1027, July 2022.

[16] C. R. Wottawa, B. Genovese, B. N. Nowroozi, S. D. Hart, J. W. Bisley, W. S. Grundfest, and E. P. Dutson, "Evaluating tactile feedback in robotic surgery for potential clinical application using an animal model," *Surg. Endosc.,* vol. 30, no. 8, pp. 3198-209, Aug. 2016.

[17] B. Tang, G. B. Hanna, and A. Cuschieri, "Analysis of errors enacted by surgical trainees during skills training courses," *Surgery,* vol. 138, no. 1, pp. 14-20, July 2005.

[18] A. H. Hadi Hosseinabadi, and S. E. Salcudean, "Force sensing in robot-assisted keyhole endoscopy: A systematic survey," *Int. J. Rob. Res.,* vol. 41, no. 2, pp. 136-162, 2021.

[19] W. Wang, J. Wang, Y. Luo, X. Wang, and H. Song, "A Survey on Force Sensing Techniques in Robot-Assisted Minimally Invasive Surgery," *IEEE Trans. Haptics,* vol. 16, no. 4, pp. 702-718, Oct.-Dec. 2023.

[20] A. L. Trejos, R. V. Patel, and M. D. Naish, "Force sensing and its application in minimally invasive surgery and therapy: A survey," *Proc. IMechE Part C: J. Mechanical Engineering Science,* vol. 224, no. 7, pp. 1435 - 1454, Jan. 2010.

[21] C. Neupert, S. Matich, N. Scherping, M. Kupnik, R. Werthschutzky, and C. Hatzfeld, "Pseudo-Haptic Feedback in Teleoperation," *IEEE Trans. Haptics,* vol. 9, no. 3, pp. 397-408, July-Sept. 2016.

[22] C. Hatzfeld, and T. A. Kern, *Engineering Haptic Devices*, p.^pp. 4-25, London, UK: Springer, 2014.

[23] S. Schostek, M. O. Schurr, and G. F. Buess, "Review on aspects of artificial tactile feedback in laparoscopic surgery," *Med. Eng. Phys.,* vol. 31, no. 8, pp. 887-98, Oct. 2009.

[24] A. Abiri, J. Pensa, A. Tao, J. Ma, Y. Y. Juo, S. J. Askari, J. Bisley, J. Rosen, E. P. Dutson, and W. S. Grundfest, "Multi-Modal Haptic Feedback for Grip Force Reduction in Robotic Surgery," *Sci. Rep.,* vol. 9, no. 1, pp. 5016, Mar. 2019.

[25] W. Othman, Z. A. Lai, C. Abril, J. S. Barajas-Gamboa, R. Corcelles, M. Kroh, and M. A. Qasaimeh, "Tactile Sensing for Minimally Invasive Surgery: Conventional Methods and Potential Emerging Tactile Technologies," *Front. Robot. AI,* vol. 8, pp. 705662, Jan. 2022.

[26] A. Abiri, Y. Y. Juo, A. Tao, S. J. Askari, J. Pensa, J. W. Bisley, E. P. Dutson, and W. S. Grundfest, "Artificial palpation in robotic surgery using haptic feedback," *Surg. Endosc.,* vol. 33, no. 4, pp. 1252-1259, Apr. 2019.

[27] M. Bergholz, M. Ferle, and B. M. Weber, "The benefits of haptic feedback in robot assisted surgery and their moderators: a meta-analysis," *Sci. Rep.,* vol. 13, no. 1, pp. 19215, Nov. 2023.

[28] Z. Li, X. Li, J. Lin, Y. Pang, D. Yang, L. Zhong, and J. Guo, "Design and Application of Multidimensional Force/Torque Sensors in Surgical Robots: A Review," *IEEE Sensors J.,* vol. 23, no. 12, pp. 12441-12454, June 2023.

[29] W. McMahan, J. Gewirtz, D. Standish, P. Martin, J. A. Kunkel, M. Lilavois, A. Wedmid, D. I. Lee, and K. J. Kuchenbecker, "Tool Contact Acceleration Feedback for Telerobotic Surgery," *IEEE Trans. Haptics,* vol. 4, no. 3, pp. 210-20, May-June 2011.

[30] A. A. Nazari, F. Janabi-Sharifi, and K. Zareinia, "Image-Based Force Estimation in Medical Applications: A Review," *IEEE Sensors J.,* vol. 21, no. 7, pp. 8805-8830, Apr. 2021.

[31] J. Hao, D. Song, C. Hu, and C. Shi, "Two-Dimensional Shape and Distal Force Estimation for the Continuum Robot Based on Learning From the Proximal Sensors," *IEEE Sensors J.,* vol. 23, no. 10, pp. 10836-10846, May. 2023.

[32] R. Xue, Z. Du, Z. Yan, and B. Ren, "An estimation method of grasping force for laparoscope surgical robot based on the model of a cable-pulley system," *Mech. Mach. Theory.,* vol. 134, pp. 440-454, Apr. 2019.

[33] M. S. Raghu Prasad, S. Purswani, and M. Manivannan, "Force JND for Right Index Finger Using Contra Lateral Force Matching Paradigm," in ICoRD'13, 2013, pp. 365-375.

[34] S. Kim, C. Kim, S. Park, and D. Y. Lee, "A 3-DOF sensor to estimate the force applied to the tip of a surgical instrument," in 2017 18th International Conference on Advanced Robotics (ICAR), 2017, pp. 143-148.

[35] Z. Tang, S. Wang, M. Li, and C. Shi, "Development of a Distal Tri-Axial Force Sensor for Minimally Invasive Surgical Palpation," *IEEE Trans. Med. Robot. Bionics,* vol. 4, no. 1, pp. 145-155, Feb. 2022.

[36] K. Li, B. Pan, J. Zhan, W. Gao, Y. Fu, and S. Wang, "Design and performance evaluation of a 3-axis force sensor for MIS palpation," *Sensor Rev.,* vol. 35, no. 2, pp. 219-228, Mar. 2015.

[37] A. L. Trejos, A. Escoto, D. Hughes, M. D. Naish, and R. V. Patel, "A sterilizable force-sensing instrument for laparoscopic surgery," *5th IEEE RAS/EMBS International Conference on Biomedical Robotics and Biomechatronics*, pp. 157-162, 2014.

[38] A. J. Spiers, H. J. Thompson, and A. G. Pipe, "Investigating remote sensor placement for practical haptic sensing with EndoWrist surgical tools," in 2015 IEEE World Haptics Conference, 2015, pp. 152-157.

[39] C. Shi, X. Luo, J. Guo, Z. Najdovski, T. Fukuda, and H. Ren, "Three-Dimensional Intravascular Reconstruction Techniques Based on Intravascular Ultrasound: A Technical Review," *IEEE J. Biomed. Health Inform.,* vol. 22, no. 3, pp. 806-817, May 2018.

[40] R. Xue, B. Ren, J. Huang, Z. Yan, and Z. Du, "Design and Evaluation of FBG-Based Tension Sensor in Laparoscope Surgical Robots," *Sensors (Basel),* vol. 18, no. 7, June 2018.

[41] F. Anooshahpour, I. G. Polushin, and R. V. Patel, “Quasi-static modeling of the da Vinci instrument,” in 2014 IEEE/RSJ International Conference on Intelligent Robots and Systems, 2014, pp. 1308-1313.
[42] N. Bandari, J. Dargahi, and M. Packirisamy, “Tactile Sensors for Minimally Invasive Surgery: A Review of the State-of-the-Art, Applications, and Perspectives,” *IEEE Access,* vol. 8, pp. 7682-7708, Dec. 2020.
[43] H. Shi, B. Zhang, X. Mei, and Q. Song, “Realization of Force Detection and Feedback Control for Slave Manipulator of Master/Slave Surgical Robot,” *Sensors (Basel),* vol. 21, no. 22, Nov. 2021.
[44] J. B. Gafford, S. B. Kesner, R. J. Wood, and C. J. Walsh, “Force-sensing surgical grasper enabled by pop-up book MEMS,” in 2013 IEEE/RSJ International Conference on Intelligent Robots and Systems, 2013, pp. 2552-2558.
[45] C. H. King, M. O. Culjat, M. L. Franco, C. E. Lewis, E. P. Dutson, W. S. Grundfest, and J. W. Bisley, “Tactile Feedback Induces Reduced Grasping Force in Robot-Assisted Surgery,” *IEEE Trans. Haptics,* vol. 2, no. 2, pp. 103-110, Apr.-June 2009.
[46] S. Schostek, C. N. Ho, D. Kalanovic, and M. O. Schurr, “Artificial tactile sensing in minimally invasive surgery - a new technical approach,” *Minim. Invasive Ther. Allied. Technol.,* vol. 15, no. 5, pp. 296-304, 2006.
[47] D. H. Lee, U. Kim, H. Moon, J. C. Koo, W. J. Yoon, and H. R. Choi, “Preliminary design of multi-axial contact force sensor for minimally invasive robotic surgery grasper,” in 2013 IEEE International Conference on Robotics and Automation, 2013, pp. 1019-1024.
[48] U. Kim, Y. B. Kim, J. So, D.-Y. Seok, and H. R. Choi, “Sensorized Surgical Forceps for Robotic-Assisted Minimally Invasive Surgery,” *IEEE Trans. Ind. Electron.,* vol. 65, no. 12, pp. 9604-9613, Dec. 2018.
[49] A. Rivadeneyra, and J. A. Lopez-Villanueva, “Recent Advances in Printed Capacitive Sensors,” *Micromachines,* vol. 11, no. 4, pp. 367, Apr. 2020.
[50] M.-L. Hsieh, S.-K. Yeh, J.-H. Lee, M.-C. Cheng, and W. Fang, “CMOS-MEMS capacitive tactile sensor with vertically integrated sensing electrode array for sensitivity enhancement,” *Sens. Actuators A Phys.,* vol. 317, pp. 112350, Jan. 2021.
[51] S. Sokhanvar, M. Packirisamy, and J. Dargahi, “MEMS Endoscopic Tactile Sensor: TowardIn-SituandIn-VivoTissue Softness Characterization,” *IEEE Sensors J.,* vol. 9, no. 12, pp. 1679-1687, Oct. 2009.
[52] N. M. Bandari, R. Ahmadi, A. Hooshiar, J. Dargahi, and M. Packirisamy, “Hybrid piezoresistive-optical tactile sensor for simultaneous measurement of tissue stiffness and detection of tissue discontinuity in robot-assisted minimally invasive surgery,” *J. Biomed. Opt.,* vol. 22, no. 7, pp. 77002, July 2017.
[53] L. Zhang, F. Ju, Y. Cao, Y. Wang, and B. Chen, “A tactile sensor for measuring hardness of soft tissue with applications to minimally invasive surgery,” *Sens. Actuators A Phys.,* vol. 266, pp. 197-204, Oct. 2017.
[54] P. Polygerinos, L. D. Seneviratne, R. Razavi, T. Schaeffter, and K. Althoefer, “Triaxial Catheter-Tip Force Sensor for MRI-Guided Cardiac Procedures,” *IEEE ASME Trans. Mechatron,* vol. 18, no. 1, pp. 386-396, Feb. 2013.
[55] X. Hui, L. Hongbin, L. D. Seneviratne, and K. Althoefer, “An Optical Tactile Array Probe Head for Tissue Palpation During Minimally Invasive Surgery,” *IEEE Sensors J.,* vol. 14, no. 9, pp. 3283-3291, July 2014.
[56] N. Bandari, J. Dargahi, and M. Packirisamy, “Miniaturized Optical Force Sensor for Minimally Invasive Surgery With Learning-Based Nonlinear Calibration,” *IEEE Sensors J.,* vol. 20, no. 7, pp. 3579-3592, Apr. 2020.
[57] Z. Mo, W. Xu, and N. G. R. Broderick, “Capability Characterization via Ex-vivo Experiments of a Fiber Optical Tip Force Sensing Needle for Tissue Identification,” *IEEE Sensors J.,* vol. 18, no. 3, pp. 1195-1202, Nov. 2017.
[58] H. Su, W. Shang, G. Li, N. Patel, and G. S. Fischer, “An MRI-Guided Telesurgery System Using a Fabry-Perot Interferometry Force Sensor and a Pneumatic Haptic Device,” *Ann. Biomed. Eng.,* vol. 45, no. 8, pp. 1917-1928, Aug 2017.
[59] L. Xiao, T. Yang, B. Huo, X. Zhao, J. Han, and W. Xu, “Impedance control of a robot needle with a fiber optic force sensor,” in 2016 IEEE 13th International Conference on Signal Processing (ICSP), 2016, pp. 1379-1383.
[60] Q. Liu, Y. Dai, M. Li, B. Yao, and J. Zhang, “FBG-Based Sensorized Surgical Instrument for Force Measurement in Minimally Invasive Robotic Surgery,” *IEEE Sensors J.,* vol. 24, no. 7, pp. 11450-11458, Apr. 2024.
[61] T. Li, C. Shi, and H. Ren, “A High-Sensitivity Tactile Sensor Array Based on Fiber Bragg Grating Sensing for Tissue Palpation in Minimally Invasive Surgery,” *IEEE/ASME Trans. Mechatronics,* vol. 23, no. 5, pp. 2306-2315, Oct. 2018.
[62] T. Li, F. Chen, Z. Zhao, Q. Pei, Y. Tan, and Z. Zhou, “Hybrid Data-Driven Optimization Design of a Layered Six-Dimensional FBG Force/Moment Sensor With Gravity Self-Compensation for Orthopedic Surgery Robot,” *IEEE Trans. Ind. Electron.,* vol. 70, no. 8, pp. 8568-8579, Aug. 2023.
[63] C. He, S. Wang, H. Sang, J. Li, and L. Zhang, “Force sensing of multiple-DOF cable-driven instruments for minimally invasive robotic surgery,” *Int. J. Med. Robotics Comput. Assist. Surg.,* vol. 10, no. 3, pp. 314-24, Sept. 2014.
[64] H. Wang, Z. Yan, Y. Gao, W. Wang, and Z. Du, “3-D Force Sensing Strategy of Laryngeal Continuum Surgical Robot Based on Fiber Bragg Gratings,” *IEEE Trans. Instrum. Meas.,* vol. 70, pp. 1-10, Aug. 2021.
[65] C. Lv, S. Wang, and C. Shi, “A High-Precision and Miniature Fiber Bragg Grating-Based Force Sensor for Tissue Palpation During Minimally Invasive Surgery,” *Ann. Biomed. Eng.,* vol. 48, no. 2, pp. 669-681, Feb. 2020.
[66] U. Kim, Y. B. Kim, D.-Y. Seok, and H. R. Choi, "S-Surge: A Portable Surgical Robot Based on a Novel Mechanism With Force-Sensing Capability for Robotic Surgery," *Handbook of Robotic and Image-Guided Surgery*, pp. 265-283: Elsevier, 2020.
[67] K. Li, B. Pan, F. Zhang, W. Gao, Y. Fu, and S. Wang, “A novel 4-DOF surgical instrument with modular joints and 6-Axis Force sensing capability,” *Int. J. Med. Robotics Comput. Assist. Surg.,* vol. 13, no. 1, May 2017.
[68] K. Sun, M. Li, S. Wang, G. Zhang, H. Liu, and C. Shi, “Development of a Fiber Bragg Grating-Enabled Clamping Force Sensor Integrated on a Grasper for Laparoscopic Surgery,” *IEEE Sensors J.,* vol. 21, no. 15, pp. 16681-16690, Aug. 2021.
[69] D.-Y. Seok, Y. B. Kim, U. Kim, S. Y. Lee, and H. R. Choi, “Compensation of Environmental Influences on Sensorized-Forceps for Practical Surgical Tasks,” *IEEE Rob. Autom. Lett.,* vol. 4, no. 2, pp. 2031-2037, Apr. 2019.
[70] L. Yu, Y. Yan, X. Yu, and Y. Xia, “Design and Realization of Forceps With 3-D Force Sensing Capability for Robot-Assisted Surgical System,” *IEEE Sensors J.,* vol. 18, no. 21, pp. 8924-8932, Nov. 2018.
[71] D. Callaghan, G. Rajan, M. McGrath, E. Coyle, Y. Semenova, and G. Farrell, “Comparing FBG and PCF Force Sensors in a Laparoscopic Smart Surgical Scissor Instrument,” in Proceedings of the 2011 SCATh Joint Workshop on New Technologies for Computer/Robot Assisted Surgery, 2011, pp. 1-4.
[72] A. Bicchi, G. Canepa, D. D. Rossi, P. Iacconi, and E. P. Scilingo, “A sensor-based minimally invasive surgery tool for detecting tissutal elastic properties,” in Proceedings of IEEE International Conference on Robotics and Automation, 1996, pp. 884-888.
[73] E. P. Scilingo, D. D. Rossi, A. Bicchi, and P. Iacconi, “Sensors and devices to enhance the performances of a minimally invasive surgery tool for replicating surgeon's haptic perception of the manipulated tissues,” in Proceedings of the 19th Annual International Conference of the IEEE Engineering in Medicine and Biology Society, 1997, pp. 961-964.
[74] S. K. Prasad, M. Kitagawa, G. S. Fischer, J. Zand, M. A. Talamini, R. H. Taylor, and A. M. Okamura, “A Modular 2-DOF Force-Sensing Instrument For Laparoscopic Surgery,” in Medical Image Computing and Computer-Assisted Intervention, 2003, pp. 279–286.
[75] H. Mayer, F. Gomez, D. Wierstra, I. Nagy, A. Knoll, and J. Schmidhuber, “A System for Robotic Heart Surgery that Learns to Tie Knots Using Recurrent Neural Networks,” in 2006 IEEE/RSJ International Conference on Intelligent Robots and Systems, 2006, pp. 543-548.
[76] G. Tholey, and J. P. Desai, “A Modular, Automated Laparoscopic Grasper with Three-Dimensional Force Measurement Capability,” in Proceedings 2007 IEEE International Conference on Robotics and Automation, 2007, pp. 250-255.
[77] G. Tholey, and J. P. Desai, “A Compact and Modular Laparoscopic Grasper With Tridirectional Force Measurement Capability,” *J. Med. Device,* vol. 2, no. 3, pp. 031001, Sept. 2008.
[78] M. M. Dalvand, B. Shirinzadeh, N. Saeid, F. Karimirad, and J. Smith, “Force measurement capability for robotic assisted minimally invasive surgery systems,” in Proceedings of the World Congress on Engineering and Computer Science, 2013.

[79] M. Moradi Dalvand, B. Shirinzadeh, A. H. Shamdani, J. Smith, and Y. Zhong, “An actuated force feedback enabled laparoscopic instrument for robotiƒ assisted surgery,” *Int. J. Med. Robotics Comput. Assist. Surg.,* vol. 10, pp. 11-21, May 2014.

[80] A. L. Trejos, R. V. Patel, M. D. Naish, A. C. Lyle, and C. M. Schlachta, “A Sensorized Instrument for Skills Assessment and Training in Minimally Invasive Surgery,” *J. Med. Devices,* vol. 3, no. 4, pp. 041002, Dec. 2009.

[81] S. Shimachi, Y. Fujiwara, and Y. Hakozaki, “New sensing method of force acting on instrument for laparoscopic robot surgery,” *Int. Congr. Ser.,* vol. 1268, pp. 775-780, June 2004.

[82] S. Shimachi, F. Kameyama, Y. Hakozaki, and Y. Fujiwara, “Contact force measurement of instruments for force-feedback on a surgical robot: acceleration force cancellations based on acceleration sensor readings,” *Med. Image. Comput. Comput. Assist. Interv.,* vol. 8, no. Pt 2, pp. 97-104, 2005.

[83] S. Shimachi, S. Hirunyanitiwatna, Y. Fujiwara, A. Hashimoto, and Y. Hakozaki, “Adapter for contact force sensing of the da Vinci robot,” *Int. J. Med. Robot,* vol. 4, no. 2, pp. 121-30, June 2008.

[84] S. Shimachi, Y. Hakozaki, T. Tada, and Y. Fujiwara, “Measurement of force acting on surgical instrument for force-feedback to master robot console,” *Int. Congr. Ser.,* vol. 1256, pp. 538-546, June 2003.

[85] J. Jiang, L. Xie, and H. L. Yu, “A 6-Axis Sensor for Minimally Invasive Robotic Surgery,” in International Conference on Intelligent Robotics and Applications, 2013, pp. 429-435.

[86] J.-F. Jiang, L. Xie, Y. Hailong, W. Yu, and B. Wu, “Development of a six-dimensional sensor for minimally invasive robotic surgery,” *J. Mech. Med. Biol.,* vol. 14, no. 5, pp. 1450074, Oct. 2014.

[87] H. Yu, J. Jiang, L. Xie, L. Liu, Y. Shi, and P. Cai, “Design and static calibration of a six-dimensional force/torque sensor for minimally invasive surgery,” *Minim. Invasive. Ther. Allied. Technol.,* vol. 23, no. 3, pp. 136-43, June 2014.

[88] U. Seibold, B. Kübler, H. Weiss, T. Ortmaier, and G. Hirzinger, “Sensorized and Actuated Instruments for Minimally Invasive Robotic Surgery,” 2004.

[89] B. Kuebler, U. Seibold, and G. Hirzinger, “Development of actuated and sensor integrated forceps for minimally invasive robotic surgery,” *Int. J. Med. Robot,* vol. 1, no. 3, pp. 96-107, Sept. 2005.

[90] U. Seibold, B. Kubler, and G. Hirzinger, “Prototype of Instrument for Minimally Invasive Surgery with 6-Axis Force Sensing Capability," in Proceedings of the IEEE International Conference on Robotics and Automation, 2005, pp. 496-501.

[91] U. Hagn, T. Ortmaier, R. Konietschke, B. Kubler, U. Seibold, A. Tobergte, M. Nickl, S. Jorg, and G. Hirzinger, “Telemanipulator for remote minimally invasive surgery,” *IEEE Robot. Automat. Mag.,* vol. 15, no. 4, pp. 28-38, June 2008.

[92] K. Li, B. Pan, W.-p. Gao, H.-b. Feng, Y.-l. Fu, and S.-g. Wang, “Miniature 6-axis force/torque sensor for force feedback in robot-assisted minimally invasive surgery," *J. Cent. South Univ.,* vol. 22, no. 12, pp. 4566-4577, Dec. 2015.

[93] S. Matich, M. Hessinger, M. Kupnik, R. Werthschützky, and C. Hatzfeld, “Miniaturized multi-axial force/torque sensor with a rollable hexapod structure,” *TM-Tech. Mess.,* vol. 84, no. s1, pp. 138-142, 2017.

[94] M. B. Schäfer, A. M. Glöckner, G. R. Friedrich, J. G. Meiringer, and P. P. Pott, “Measuring interaction forces in surgical telemanipulation using conventional instruments,” *Robotica,* vol. 41, no. 4, pp. 1335-1347, Dec. 2022.

[95] I. Brouwer, J. Ustin, L. Bentley, A. Sherman, N. Dhruv, and F. Tendick, “Measuring in vivo animal soft tissue properties for haptic modeling in surgical simulation,” *Stud. Health. Technol. Inform.,* vol. 81, pp. 69-74, Feb. 2001.

[96] J. D. Brown, J. Rosen, M. Moreyra, M. Sinanan, and B. Hannaford, “Computer-controlled motorized endoscopic grasper for in vivo measurement of soft tissue biomechanical characteristics,” *Stud. Health. Technol. Inform.,* vol. 85, pp. 71-73, Apr. 2002.

[97] J. D. Brown, J. Rosen, Y. S. Kim, L. Chang, M. N. Sinanan, and B. Hannaford, “In-vivo and in-situ compressive properties of porcine abdominal soft tissues,” *Stud. Health. Technol. Inform.,* vol. 94, pp. 26-32, Apr. 2003.

[98] S. Matich, C. Neupert, A. Kirschniak, H. F. Schlaak, and P. Pott, “3-D force measurement using single axis force sensors in a new single port parallel kinematics surgical manipulator,” in 2016 IEEE/RSJ International Conference on Intelligent Robots and Systems (IROS), 2016, pp. 3665-3670.

[99] G. Tholey, A. Pillarisetti, and J. P. Desai, "On-site three dimensional force sensing capability in a laparoscopic grasper," *Ind. Rob.,* vol. 31, no. 6, pp. 509-518, Dec. 2004.

[100] G. Tholey, A. Pillarisetti, W. Green, and J. P. Desai, “Design, Development, and Testing of an Automated Laparoscopic Grasper with 3-D Force Measurement Capability,” in Medical Simulation: International Symposium, 2004, pp. 38-48.

[101] G. S. Fischer, T. Akinbiyi, S. Saha, J. Zand, M. Talamini, M. Marohn, and R. Taylor, “Ischemia and Force Sensing Surgical Instruments for Augmenting Available Surgeon Information,” in The First IEEE/RAS-EMBS International Conference on Biomedical Robotics and Biomechatronics, 2006, pp. 1030-1035.

[102] M. Stephan, G. Rognini, A. Sengul, R. Beira, L. Santos-Carreras, and H. Bleuler, “Modeling and design of a gripper for a robotic surgical system integrating force sensing capabilities in 4 DOF,” in ICCAS 2010, 2010, pp. 361-365.

[103] M. B. Hong, and Y.-H. Jo, “Design and Evaluation of 2-DOF Compliant Forceps With Force-Sensing Capability for Minimally Invasive Robot Surgery,” *IEEE Trans. Robot.,* vol. 28, no. 4, pp. 932-941, Aug. 2012.

[104] L. Yu, Y. Yan, C. Li, and X. Zhang, “Three-dimensional nonlinear force-sensing method based on double microgrippers with E-type vertical elastomer for minimally invasive robotic surgery,” *Robotica,* vol. 36, no. 6, pp. 865-881, Jan. 2018.

[105] C. Hou, J. Geng, Y. Sun, T. Chen, F. Wang, H. Ren, X. Zuo, Y. Li, H. Liu, and L. Sun, “A sensorised forcep based on piezoresistive force sensor for robotic-assisted minimally invasive surgery,” in 2021 IEEE 16th International Conference on Nano/Micro Engineered and Molecular Systems (NEMS), 2021, pp. 60-63.

[106] A. L. Trejos, A. Escoto, M. D. Naish, and R. V. Patel, “Design and Evaluation of a Sterilizable Force Sensing Instrument for Minimally Invasive Surgery,” *IEEE Sensors J.,* vol. 17, no. 13, pp. 3983-3993, July 2017.

[107] W. J. Peine, J. S. Son, and R. D. Howe, “A palpation system for artery localization in laparoscopic surgery,” in First International Symposium on Medical Robotics and Computer-Assisted Surgery, Pittsburgh, 1994, pp. 22-24.

[108] R. D. Howe, W. J. Peine, D. A. Kantarinis, and J. S. Son, “Remote palpation technology,” *IEEE Eng. Med. Biol. Mag.,* vol. 14, no. 3, pp. 318-323, May-June 1995.

[109] D. T. Pawluk, J. S. Son, P. S. Wellman, W. J. Peine, and R. D. Howe, “A distributed pressure sensor for biomechanical measurements,” *J. Biomech. Eng.,* vol. 120, no. 2, pp. 302-5, Apr. 1998.

[110] O. H. Paydar, C. R. Wottawa, R. E. Fan, E. P. Dutson, W. S. Grundfest, M. O. Culjat, and R. N. Candler, “Fabrication of a thin-film capacitive force sensor array for tactile feedback in robotic surgery,” in 2012 Annual International Conference of the IEEE Engineering in Medicine and Biology Society, 2012, pp. 2355-2358.

[111] P. Peng, R. Rajamani, and A. G. Erdman, “Flexible Tactile Sensor for Tissue Elasticity Measurements,” *J. Microelectromech Syst.,* vol. 18, no. 6, pp. 1226-1233, Dec. 2009.

[112] M. V. Ottermo, M. Ovstedal, T. Lango, O. Stavdahl, Y. Yavuz, T. A. Johansen, and R. Marvik, “The role of tactile feedback in laparoscopic surgery,” *Surg. Laparosc. Endosc. Percutan. Tech.,* vol. 16, no. 6, pp. 390-400, Dec. 2006.

[113] A. L. Trejos, J. Jayender, M. T. Perri, M. D. Naish, R. V. Patel, and R. A. Malthaner, “Robot-assisted Tactile Sensing for Minimally Invasive Tumor Localization,” *Int. J. Rob. Res.,* vol. 28, no. 9, pp. 1118-1133, Sept. 2009.

[114] A. Talasaz, and R. V. Patel, “Integration of force reflection with tactile sensing for minimally invasive robotics-assisted tumor localization,” *IEEE Trans. Haptics,* vol. 6, no. 2, pp. 217-28, Apr.-June 2013.

[115] A. S. Naidu, A. Escoto, O. Fahmy, R. V. Patel, and M. D. Naish, “An autoclavable wireless palpation instrument for minimally invasive surgery,” in 2016 38th Annual International Conference of the IEEE Engineering in Medicine and Biology Society (EMBC), 2016, pp. 6489-6492.

[116] A. S. Naidu, R. V. Patel, and M. D. Naish, “Low-Cost Disposable Tactile Sensors for Palpation in Minimally Invasive Surgery,” *IEEE/ASME Trans. Mechatronics,* vol. 22, no. 1, pp. 127-137, Feb. 2017.

[117] Y. Dai, A. Abiri, S. Liu, O. Paydar, H. Sohn, E. P. Dutson, W. S. Grundfest, and R. N. Candler, “Grasper integrated tri-axial force sensor system for robotic minimally invasive surgery,” in 2017 39th Annual International Conference of the IEEE Engineering in Medicine and Biology Society (EMBC), 2017, pp. 3936-3939.

[118] Y. Dai, "Grasper Integrated Miniaturized Tri-Axial Force Sensor System for Robotic Minimally Invasive Surgery," Ph.D., Doctor of Philosophy in Electrical and Computer Engineering, University of California, Los Angeles, 2018.
[119] U. Kim, D.-H. Lee, Y. B. Kim, D.-Y. Seok, J. So, and H. R. Choi, "S-Surge: Novel Portable Surgical Robot with Multiaxis Force-Sensing Capability for Minimally Invasive Surgery," *IEEE/ASME Trans. Mechatronics,* vol. 22, no. 4, pp. 1717-1727, Aug. 2017.
[120] U. Kim, D. H. Lee, H. Moon, J. C. Koo, and H. R. Choi, "Design and realization of grasper-integrated force sensor for minimally invasive robotic surgery," in 2014 IEEE/RSJ International Conference on Intelligent Robots and Systems, 2014, pp. 4321-4326.
[121] U. Kim, D.-H. Lee, W. J. Yoon, B. Hannaford, and H. R. Choi, "Force Sensor Integrated Surgical Forceps for Minimally Invasive Robotic Surgery," *IEEE Trans. Robot.,* vol. 31, no. 5, pp. 1214-1224, Sept. 2015.
[122] U. Kim, Y. B. Kim, D. Seok, J. So, and H. R. Choi, "A new type of surgical forceps integrated with three-axial force sensor for minimally invasive robotic surgery," in 2016 13th International Conference on Ubiquitous Robots and Ambient Intelligence (URAI), 2016, pp. 135-137.
[123] U. Kim, Y. B. Kim, D. Y. Seok, J. So, and H. R. Choi, "Development of surgical forceps integrated with a multi-axial force sensor for minimally invasive robotic surgery," in 2016 IEEE/RSJ International Conference on Intelligent Robots and Systems (IROS), 2016, pp. 3684-3689.
[124] D.-H. Lee, U. Kim, and H. R. Choi, "Development of multi-axial force sensing system for haptic feedback enabled minimally invasive robotic surgery," in 2014 IEEE/RSJ International Conference on Intelligent Robots and Systems, 2014, pp. 4309-4314.
[125] H.-R. Choi, D.-H. Lee, U. Kim, T. Gulrez, W. J. Yoon, and B. Hannaford, "A Laparoscopic Grasping Tool with Force Sensing Capability," *IEEE/ASME Trans. Mechatronics,* vol. 21, no. 1, pp. 130-141, June 2015.
[126] U. Kim, Y. B. Kim, D.-Y. Seok, J. So, and H. R. Choi, "A Surgical Palpation Probe With 6-Axis Force/Torque Sensing Capability for Minimally Invasive Surgery," *IEEE Trans. Ind. Electron.,* vol. 65, no. 3, pp. 2755-2765, Mar. 2018.
[127] C.-H. Mak, Y. Li, K. Wang, M. Wu, J. D.-L. Ho, Q. Dou, K.-Y. Sze, K. Althoefer, and K.-W. Kwok, "Intelligent Shape Decoding of a Soft Optical Waveguide Sensor," *Adv. Intell. Syst.,* vol. 6, no. 2, pp. 2300082, July 2023.
[128] W. Li, J. Konstantinova, Y. Noh, Z. Ma, A. Alomainy, and K. Althoefer, "An Elastomer-based Flexible Optical Force and Tactile Sensor," in 2019 2nd IEEE International Conference on Soft Robotics (RoboSoft), 2019, pp. 361-366.
[129] C. Shang, B. Fu, J. Tuo, X. Guo, Z. Li, Z. Wang, L. Xu, and J. Guo, "Soft Biomimetic Fiber-Optic Tactile Sensors Capable of Discriminating Temperature and Pressure," *ACS Appl. Mater. Interfaces,* vol. 15, no. 46, pp. 53264-53272, Nov. 2023.
[130] T. Li, A. Pan, and H. Ren, "Reaction Force Mapping by 3-Axis Tactile Sensing With Arbitrary Angles for Tissue Hard-Inclusion Localization," *IEEE Trans. Biomed. Eng.,* vol. 68, no. 1, pp. 26-35, Jan. 2021.
[131] T. Li, J. Guo, H. Zheng, S. Wang, L. Qiu, and H. Ren, "Fault-Tolerant Six-Axis FBG Force/Moment Sensing for Robotic Interventions," *IEEE/ASME Trans. Mechatronics,* vol. 28, no. 6, pp. 3537-3550, Dec. 2023.
[132] H. Su, M. Zervas, G. A. Cole, C. Furlong, and G. S. Fischer, "Real-time MRI-guided needle placement robot with integrated fiber optic force sensing," *2011 IEEE International Conference on Robotics and Automation*, pp. 1583-1588, 2011.
[133] Z. Mo, and W. Xu, "Temperature-Compensated Optical Fiber Force Sensing at the Tip of a Surgical Needle," *IEEE Sensors J.,* vol. 16, no. 24, pp. 8936-8943, Dec. 2016.
[134] J. Peirs, J. Clijnen, D. Reynaerts, H. V. Brussel, P. Herijgers, B. Corteville, and S. Boone, "A micro optical force sensor for force feedback during minimally invasive robotic surgery," *Sens. Actuators A Phys.,* vol. 115, no. 2-3, pp. 447-455, Sept. 2004.
[135] P. Puangmali, L. Hongbin, L. D. Seneviratne, P. Dasgupta, and K. Althoefer, "Miniature 3-Axis Distal Force Sensor for Minimally Invasive Surgical Palpation," *IEEE/ASME Trans. Mechatronics,* vol. 17, no. 4, pp. 646-656, May 2012.
[136] H. Xie, A. Jiang, H. A. Wurdemann, H. Liu, L. D. Seneviratne, and K. Althoefer, "Magnetic Resonance-Compatible Tactile Force Sensor Using Fiber Optics and Vision Sensor," *IEEE Sensors J.,* vol. 14, no. 3, pp. 829-838, Jan. 2014.
[137] X. Hui, L. Hongbin, L. Shan, L. D. Seneviratne, and K. Althoefer, "Fiber optics tactile array probe for tissue palpation during minimally invasive surgery," in 2013 IEEE/RSJ International Conference on Intelligent Robots and Systems, 2013, pp. 2539-2544.
[138] S. B. Kesner, and R. D. Howe, "Design Principles for Rapid Prototyping Forces Sensors using 3D Printing," *IEEE ASME Trans. Mechatronics,* vol. PP, no. 99, pp. 1-5, July 2011.
[139] F. Taffoni, D. Formica, P. Saccomandi, G. Di Pino, and E. Schena, "Optical fiber-based MR-compatible sensors for medical applications: an overview," *Sensors (Basel),* vol. 13, no. 10, pp. 14105-20, Oct. 2013.
[140] M. S. Müller, L. Hoffmann, T. Christopher Buck, and A. Walter Koch, "Fiber Bragg grating-based force-torque sensor with six degrees of freedom," *Int. J. Optomechatronics,* vol. 3, no. 3, pp. 201-214, Sept. 2009.
[141] C. Kim, and C.-H. Lee, "Development of a 6-DoF FBG force–moment sensor for a haptic interface with minimally invasive robotic surgery," *J. Mech. Sci. Technol.,* vol. 30, no. 8, pp. 3705-3712, Aug. 2016.
[142] R. Haslinger, P. Leyendecker, and U. Seibold, "A fiberoptic force-torque-sensor for minimally invasive robotic surgery," in 2013 IEEE International Conference on Robotics and Automation, 2013, pp. 4390-4395.
[143] H. Song, K. Kim, and J. Lee, "Development of optical fiber Bragg grating force-reflection sensor system of medical application for safe minimally invasive robotic surgery," *Rev. Sci. Instrum.,* vol. 82, no. 7, pp. 074301, July 2011.
[144] I. Barukčić, H. Wang, W. Wang, Z. Du, and Y. Gao, "Design of 3D force perception system of surgical robots based on Fiber Bragg Grating," in International Conference on Computer Science Communication and Network Security (CSCNS2020), 2021.
[145] C. Du, D. Wei, H. Wang, W. Wang, J. Dong, H. Huo, and Y. Li, "Development of the X-Perce—A Universal FBG-Based Force Sensing Kit for Laparoscopic Surgical Robot," *IEEE Trans. Med. Robot. Bionics,* vol. 4, no. 1, pp. 183-193, Feb. 2022.
[146] M. D. Murphy, A. Midha, and L. L. Howell, "The topological synthesis of compliant mechanisms," *Mech. Mach. Theory.,* vol. 31, no. 2, pp. 185-199, Feb. 1996.
[147] C. Shi, M. Li, C. Lv, J. Li, and S. Wang, "A High-Sensitivity Fiber Bragg Grating-Based Distal Force Sensor for Laparoscopic Surgery," *IEEE Sensors J.,* vol. 20, no. 5, pp. 2467-2475, Mar. 2020.
[148] D. Lai, Z. Tang, J. Zhao, S. Wang, and C. Shi, "Design and Validation of a Miniature Fiber Bragg Grating-Enabled High-Sensitivity Torque Sensor," *IEEE Sensors J.,* vol. 21, no. 18, pp. 20027-20035, Sept. 2021.
[149] C. Shi, D. Lai, Z. Tang, and Z. Yang, "Development of an Optic Fiber-Based Torque Sensor With a Torsion-Translation Conversion Flexure," *IEEE Sensors J.,* vol. 22, no. 1, pp. 344-351, Jan. 2022.
[150] Z. Tang, S. Wang, and C. Shi, "Development of a Hybrid Force-Displacement Sensor Based on Fiber Bragg Grating for Radial Artery Pulse Waveform Measurement," *IEEE Sensors J.,* vol. 21, no. 18, pp. 20045-20054, Sept. 2021.
[151] C. Shi, Z. Tang, H. Zhang, and Y. Liu, "Development of an FBG-Based Wearable Sensor for Simultaneous Respiration and Heartbeat Measurement," *IEEE Trans. Instrum. Meas.,* vol. 72, pp. 1-9, Jan. 2023.
[152] C. Shi, H. Zhang, X. Ni, and K. Wang, "An FBG-Based Sensor With Both Wearable and Handheld Forms for Carotid Arterial Pulse Waveform Measurement," *IEEE Trans. Instrum. Meas.,* vol. 72, pp. 1-10, Sept. 2023.
[153] D. J. Callaghan, G. Rajan, M. M. McGrath, E. Coyle, Y. Semenova, and G. Farrell, "Investigation and experimental measurement of scissor blade cutting forces using fiber Bragg grating sensors," *Smart Mater. Struct.,* vol. 20, no. 10, pp. 105004, Aug. 2011.
[154] D. Callaghan, "Force Sensing Surgical Scissor Blades using Fibre Bragg Grating Sensors," Ph.D., School of Manufacturing and Design Engineering, Dublin Institute of Technology, Dublin, 2013.
[155] S. J. Fattahi, A. Zabihollah, and H. Adldoost, "Multi sensing grasper for minimally invasive surgery," in 2011 IEEE/ASME International Conference on Advanced Intelligent Mechatronics, 2011, pp. 344-349.
[156] J. M. López-Higuera, J. D. C. Jones, M. López-Amo, J. L. Santos, C. Ledermann, H. Pauer, and H. Woern, "Fiber optical sensor system for shape and haptics for flexible instruments in minimally invasive surgery: overview and status quo," in 23rd International Conference on Optical Fibre Sensors, 2014, pp. 915766.
[157] P. S. Zarrin, A. Escoto, R. Xu, R. V. Patel, M. D. Naish, and A. L. Trejos, "Development of an optical fiber-based sensor for grasping and axial force sensing," in 2017 IEEE International Conference on Robotics and Automation (ICRA), 2017, pp. 939-944.
[158] P. S. Zarrin, A. Escoto, R. Xu, R. V. Patel, M. D. Naish, and A. L. Trejos, "Development of a 2-DOF Sensorized Surgical Grasper for Grasping

and Axial Force Measurements," *IEEE Sensors J.,* vol. 18, no. 7, pp. 2816-2826, Apr. 2018.

[159] S. Mohith, A. R. Upadhya, K. P. Navin, S. M. Kulkarni, and M. Rao, "Recent trends in piezoelectric actuators for precision motion and their applications: a review," *Smart Mater. Struct.,* vol. 30, no. 1, Dec. 2020.

[160] X. He, M. Balicki, P. Gehlbach, J. Handa, R. Taylor, and I. Iordachita, "A multi-function force sensing instrument for variable admittance robot control in retinal microsurgery," in 2014 IEEE International Conference on Robotics and Automation (ICRA), 2014.

[161] A. Gao, B. Gonenc, J. Guo, H. Liu, P. Gehlbach, and I. Iordachita, "3-DOF force-sensing micro-forceps for robot-assisted membrane peeling: Intrinsic actuation force modeling," in 2016 6th IEEE International Conference on Biomedical Robotics and Biomechatronics, 2016, pp. 489-494.

[162] C. He, N. Patel, A. Ebrahimi, M. Kobilarov, and I. Iordachita, "Preliminary study of an RNN-based active interventional robotic system (AIRS) in retinal microsurgery," *Int. J. Comput. Assist. Radiol. Surg.,* vol. 14, no. 6, pp. 945-954, June 2019.

[163] L. Xiong, Y. Guo, G. Jiang, X. Zhou, and H. Liu, "An FBG-Based 2-DOF Force Sensing Intraocular Lens Positioning Hook for Cataract Surgery," *IEEE Photonics Technol. Lett.,* vol. 31, no. 20, pp. 1674-1677, Oct. 2019.

[164] A. Gao, Y. Zhou, L. Cao, Z. Wang, and H. Liu, "Fiber Bragg Grating-Based Triaxial Force Sensor With Parallel Flexure Hinges," *IEEE Trans. Ind. Electron.,* vol. 65, no. 10, pp. 8215-8223, Oct. 2018.

[165] T. Li, C. Shi, and H. Ren, "Three-Dimensional Catheter Distal Force Sensing for Cardiac Ablation Based on Fiber Bragg Grating," *IEEE/ASME Trans. Mechatronics,* vol. 23, no. 5, pp. 2316-2327, Oct. 2018.

[166] W. Duan, T. Akinyemi, W. Du, J. Ma, X. Chen, F. Wang, O. Omisore, J. Luo, H. Wang, and L. Wang, "Technical and Clinical Progress on Robot-Assisted Endovascular Interventions: A Review," *Micromachines,* vol. 14, no. 1, Jan. 2023.

[167] R. Ben Hassen, A. Lemmers, and A. Delchambre, "Tri-Axial Force Sensor in a Soft Catheter Using Fiber Bragg Gratings for Endoscopic Submucosal Dissection," *IEEE Sensors J.,* vol. 23, no. 20, pp. 24626-24636, Oct. 2023.

[168] T. Li, Q. Pei, A. Zhang, H. Zhou, L. Wang, Y. Tan, and Z. Zhou, "Multimode Proximal Force FBG-Based Sensors With High-Resolution for Catheter Surgical Robots," *IEEE Trans. Instrum. Meas.,* vol. 72, pp. 1-12, June 2023.

[169] C. Shi, T. Li, and H. Ren, "A Millinewton Resolution Fiber Bragg Grating-Based Catheter Two-Dimensional Distal Force Sensor for Cardiac Catheterization," *IEEE Sensors J.,* vol. 18, no. 4, pp. 1539-1546, Feb. 2018.

[170] C. Shi, S. Giannarou, S.-L. Lee, and G.-Z. Yang, "Simultaneous catheter and environment modeling for Trans-catheter Aortic Valve Implantation," in 2014 IEEE/RSJ International Conference on Intelligent Robots and Systems, 2014, pp. 2024-2029.

[171] T. Li, Q. Pei, X. Qin, Y. Liang, Y. Tan, and Z. Zhou, "Fusing the Wireless Technique Optical Fiber Force Sensor for Remote Monitoring of Sleeping Posture," *IEEE/ASME Trans. Mechatronics,* vol. 28, no. 5, pp. 2703-2715, Oct. 2023.

[172] N. V. Kumar, S. Pant, S. Sridhar, V. Marulasiddappa, S. Srivatzen, and S. Asokan, "Fiber Bragg Grating-Based Pulse Monitoring Device for Real-Time Non-Invasive Blood Pressure Measurement—A Feasibility Study," *IEEE Sensors J.,* vol. 21, no. 7, pp. 9179-9185, Apr. 2021.

[173] C. Tavares, C. Leitao, D. Lo Presti, M. F. Domingues, N. Alberto, H. Silva, and P. Antunes, "Respiratory and heart rate monitoring using an FBG 3D-printed wearable system," *Biomed. Opt. Express,* vol. 13, no. 4, pp. 2299-2311, Apr. 2022.

[174] L. Xiong, Y. Guo, G. Jiang, X. Zhou, L. Jiang, and H. Liu, "Six-Dimensional Force/Torque Sensor Based on Fiber Bragg Gratings With Low Coupling," *IEEE Trans. Ind. Electron.,* vol. 68, no. 5, pp. 4079-4089, May 2021.

[175] F. Amirabdollahian, S. Livatino, B. Vahedi, R. Gudipati, P. Sheen, S. Gawrie-Mohan, and N. Vasdev, "Prevalence of haptic feedback in robot-mediated surgery: a systematic review of literature," *J. Robot. Surg.,* vol. 12, no. 1, pp. 11-25, Mar. 2018.

[176] O. Sigmund, and K. Maute, "Topology optimization approaches," *Struct. Multidisc. Optim.,* vol. 48, no. 6, pp. 1031-1055, Aug. 2013.

[177] J. Gan, J. Zhang, M.-F. Ge, and X. Tu, "Designs of Compliant Mechanism-Based Force Sensors: A Review," *IEEE Sensors J.,* vol. 22, no. 9, pp. 8282-8294, May 2022.

[178] N. T. Tran, M. P. Dang, and T.-P. Dao, "A new optimal design synthesis method for flexure-based mechanism: recent advance of metaheuristic-based artificial intelligence for precision micropositioning system," *Microsyst. Technol.,* vol. 30, no. 1, pp. 1-31, Dec. 2023.

[179] H. Liu, T. Ji, H. Li, J. Geng, C. Hou, K. Wang, D. Li, and T. Chen, "An Integrated 3D MEMS Force Sensing and Feedback System for Robot-Assisted Minimally Invasive Surgery," *IEEE Sensors J.*, pp. 1-1, 2024.

[180] L. Meng, W. Zhang, D. Quan, G. Shi, L. Tang, Y. Hou, P. Breitkopf, J. Zhu, and T. Gao, "From Topology Optimization Design to Additive Manufacturing: Today's Success and Tomorrow's Roadmap," *Arch. Computat. Methods Eng.,* vol. 27, no. 3, pp. 805-830, Mar. 2019.